

Dynamical Symmetry Breaking in Flat Space with Non-trivial Topology

Ken-ichi Ishikawa¹, Tomohiro Inagaki², Kenji Fukazawa³, and Kazuhiro Yamamoto¹

¹*Department of Physics, Hiroshima University*

Higashi-Hiroshima 739, Japan

²*Institute for Cosmic Ray Research, University of Tokyo,*

Tanashi, Tokyo 188, Japan

³*Department of Mechanical Engineering, Kure National College of Technology,*

Kure 737, Japan

Abstract

We consider a four-fermion theory as a simple model of dynamical symmetry breaking in flat space with non-trivial topology, motivated from recent studies in similar considerations in curved space. The phase structure is investigated, by developing a useful formalism to evaluate the effective potential in arbitrary compactified flat space in 3- and 4-dimensional spacetime. The phase structure is significantly altered due to the finite volume effect in the compactified space. Interestingly, the effect works in different way depending on the boundary condition of the fermion fields. The physical interpretation of the results and its implication on the dynamical symmetry breaking phenomenon in curved space are discussed.

PACS number(s): 04.20.Gz,04.62.+v,11.30.Qc

I. INTRODUCTION

Various phenomena associated with phase transitions at the early stage of the universe have been a subject of great interest in cosmology for two decades. These phase transitions of the universe is motivated from the symmetry breaking phenomenon in high energy particle physics. One of the decisive problems in high energy particle physics is how the model of unified theories can be tested. It is expected that the primary symmetry of unified theories is broken down at the early universe to yield the theories with lower symmetries. There is a possibility to test the model at the early stage of the universe.

To investigate unified theories, much interest has been taken in clarifying the mechanism of the spontaneous symmetry breaking under the circumstance of the early universe. The dynamics of the strong coupling gauge theory may break the symmetry of the unified theories without introducing an elementary scalar field. This scenario is called as the dynamical symmetry breaking [1]. It is considered that the change of curvature or volume size of the universe may cause the dynamical symmetry breaking as the evolution of the universe proceeds. The studies of such effects on the symmetry breaking may help understanding unified theories and evolution of the early universe.

Many works have been done in this field. By using the weak curvature expansion it is found that the chiral symmetry is restored for a large positive curvature and that there is no symmetric phase in a spacetime with any negative curvature. [2–4] In weakly curved spacetime it is pointed out that non-trivial topology for the fermion field may drastically change the phase structure of the four-fermion theory. [5] The higher derivative and gauged four-fermion theories have also investigated in weakly curved spacetime. [6] In some compact spaces, e.g., de Sitter space [7,8] and Einstein universe [9], the effective potential is calculated without any approximation for the spacetime curvature. It is observed to exhibit the symmetry restoration through the second order phase transition. However, in such compact spaces, it is not clear whether the symmetry restoration is caused by the curvature or finite size effect. An example of other simple compact space with no curvature is the torus

universe. Since the torus spacetime has only the finite size effect, then the investigation in this space will indicate which effects, curvature or finite size, is essential to restore the symmetry. We therefore investigate the dynamical symmetry breaking in compact flat space with non-trivial topology.

Let us briefly comment on the cosmological motivations to consider the torus universe. Several astrophysicists have discussed the possibility of the torus universe [10–12], and recently the topology of the universe is argued by using the observational data of the cosmic microwave background anisotropies [13], which was detected by COBE DMR [14]. Assuming that our universe is the three-torus, they constrained the cell size of the torus. According to the results, the size would be larger than the present horizon scale. Thus we do not know the topology of our universe at present. Nevertheless, there are some cosmological motivations to consider compact flat space with non-trivial topology. First, quantum cosmologist have argued that small volume universe have small action, and are more likely to be created [15]. In fact, it seems difficult to create an infinite volume universe in the context of quantum cosmology. Second, the torus universe, in contrast to the compact S^3 universe, may have long lifetime because the curvature does not collapse the universe.

In this paper we make a systematic study of the dynamical symmetry breaking in compact flat space with non-trivial topology, assuming that the four-fermion theory is an effective theory which stems from more fundamental theory at GUT era. The effective potential is calculated from the Feynman propagator which depends on the spacetime structure. Evaluating the effective potential, we investigate the dynamical symmetry breaking induced by the effect of the spacetime structure. The dynamical symmetry breaking in torus universe of space-time dimension, $D = 3$, is investigated in Ref. [16–18]. Our strategy to evaluate the effective potential differs from that in Ref. [16–18]. Our method starts from the Feynman propagator in real space, then it can be easily applied to compact flat spaces with arbitrary topology for $D = 2, 3$ and 4.

The paper is organized as follows. In section 2, we show a brief review of four-fermion theory in curved space. We then extend the formalism to a useful form in order to investigate

the effective potential in compact flat space with nontrivial topology. In section 3, we apply the formalism to a 3-dimensional spacetime with nontrivial spatial sector. 4-dimensional case is investigated in section 4. Section 5 is devoted to summary and discussions. In appendix, we show the validity of our method by considering $D = 2$ case. We prove that our method leads to well known results previously obtained. We use the units $\hbar = 1$ and $c = 1$.

II. FORMALISM

In this section we first give a brief review of the four-fermion theory in curved space. We consider the system with the action [19]

$$S = \int \sqrt{-g} d^D x \left[- \sum_{k=1}^N \bar{\psi}_k \gamma^\alpha \nabla_\alpha \psi_k + \frac{\lambda_0}{2N} \left(\sum_{k=1}^N \bar{\psi}_k \psi_k \right)^2 \right], \quad (2.1)$$

where index k represents the flavors of the fermion field ψ , N is the number of fermion species, g the determinant of the metric tensor $g_{\mu\nu}$, and D the spacetime dimension. For simplicity we neglect the flavor index below.

The action (2.1) is invariant under the discrete transformation $\bar{\psi}\psi \rightarrow -\bar{\psi}\psi$. For $D = 2, 4$ this transformation is realized by the discrete chiral transformation $\psi \rightarrow \gamma_5 \psi$. Thus we call this Z^2 symmetry the discrete chiral symmetry. The discrete chiral symmetry prohibits the fermion mass term. If the composite operator constructed from the fermion and anti-fermion develops the non-vanishing vacuum expectation value, $\langle \bar{\psi}\psi \rangle \neq 0$, a fermion mass term appears in the four-fermion interaction term and the chiral symmetry is broken down dynamically.

For practical calculations in four-fermion theory it is more convenient to introduce auxiliary field σ and start with the action

$$S_y = \int \sqrt{-g} d^D x \left[-\bar{\psi} \gamma^\alpha \nabla_\alpha \psi - \frac{N}{2\lambda_0} \sigma^2 - \bar{\psi} \sigma \psi \right]. \quad (2.2)$$

The action S_y is equivalent to the action (2.1). If the non-vanishing vacuum expectation

value is assigned to the auxiliary field σ there appears a mass term for the fermion field ψ and the discrete chiral symmetry (the Z_2 symmetry) is eventually broken.

We would like to find a ground state of the system described by the four-fermion theory. For this purpose we evaluate an effective potential for the field σ . The ground state is determined by observing the minimum of the effective potential in the homogeneous and static background spacetime.

As is known, the effective potential in the leading order of the $1/N$ expansion is given by [2]

$$V(\sigma) = \frac{1}{2\lambda_0}\sigma^2 + \frac{\text{Tr}\sqrt{-g} \int_0^\sigma ds S_F(x, x'; s)}{\int d^D x \sqrt{-g}}, \quad (2.3)$$

where

$$\text{Tr} = \int \int d^D x d^D x' \delta^D(x - x') \text{tr}, \quad (2.4)$$

and $S_F(x, x'; s)$ is the Feynman propagator for free fermion with mass s , which satisfies

$$(\gamma^\alpha \nabla_\alpha + s) S_F(x, x'; s) = \frac{i}{\sqrt{-g}} \delta^D(x, x'). \quad (2.5)$$

It should be noted that the effective potential (2.3) is normalized so that $V(0) = 0$.

We introduce the Feynman propagator for the scalar field with mass s ,

$$(\square_x - s^2) G_F(x, x'; s) = \frac{i}{\sqrt{-g}} \delta^D(x, x'), \quad (2.6)$$

which has the relation,

$$S_F(x, x'; s) = (\gamma^\alpha \nabla_\alpha - s) G_F(x, x'; s). \quad (2.7)$$

Then, we write the effective potential as

$$V(\sigma) = \frac{1}{2\lambda_0}\sigma^2 - \lim_{x' \rightarrow x} \text{tr} \mathbf{1} \int_0^\sigma ds s G_F(x, x'; s), \quad (2.8)$$

in flat spacetime. Here $\text{tr} \mathbf{1}$ is the trace of an unit Dirac matrix.

Now we consider the Feynman propagator on compact flat space with nontrivial topology. We write the Feynman propagator in the D -dimensional Minkowski space as $\tilde{G}_F(x, x'; s) =$

$\tilde{G}(\xi)$, where $\xi = (x - x')^2 = (t - t')^2 - (\mathbf{x} - \mathbf{x}')^2$ and the explicit expression is given by Eq.(2.11). That is, $\tilde{G}_F(x, x'; s)$ has the Lorentz invariance, and is a function of the variable ξ . Then the Feynman propagator on the $(D - 1)$ -dimensional spatial torus whose size is $\mathbf{L} = (L_1, L_2, \dots, L_{D-1})$ can be written

$$G_F(x, x'; s) = \sum_{n_1=-\infty}^{\infty} \sum_{n_2=-\infty}^{\infty} \cdots \sum_{n_{D-1}=-\infty}^{\infty} \alpha(\mathbf{n}) \tilde{G}(\xi_{\mathbf{n}}) \equiv \sum_{\mathbf{n}} \alpha(\mathbf{n}) \tilde{G}(\xi_{\mathbf{n}}), \quad (2.9)$$

where

$$\xi_{\mathbf{n}} = (t - t')^2 - \sum_{i=1}^{D-1} (x_i - x'_i + n_i L_i)^2, \quad (2.10)$$

$\mathbf{n} = (n_1, n_2, \dots, n_{D-1})$, and $\alpha(\mathbf{n})$ is a phase factor which is determined in accordance with the boundary condition of quantum fields (see below). Throughout this paper we use a convention $x = (t, \mathbf{x}) = (t, x_1, x_2, \dots, x_{D-1})$, $x' = (t', \mathbf{x}') = (t', x'_1, x'_2, \dots, x'_{D-1})$, etc. Note that the Green function constructed in this way has the invariance under the replacement $x_i \rightarrow x_i + L_i$, and satisfies the equation of motion. *

The Feynman propagator in the D -dimensional Minkowski space is (see e.g. [20])

$$\tilde{G}_F(x, x'; s) = \tilde{G}(\xi) = \frac{\pi}{(4\pi i)^{D/2}} \left(\frac{4s^2}{-\xi + i\epsilon} \right)^{(D-2)/4} H_{D/2-1}^{(2)}([s^2(\xi - i\epsilon)]^{1/2}), \quad (2.11)$$

where $H_{\nu}^{(2)}(z)$ is the Hankel function of the second kind.

Then the effective potential is obtained by substituting Eq.(2.11) with (2.10), and (2.9) into Eq.(2.8). Performing the integration we get

$$V = \frac{1}{2\lambda_0} \sigma^2 - \lim_{x' \rightarrow x} \text{tr} \mathbf{1} \sum_{\mathbf{n}} \alpha(\mathbf{n}) \frac{\pi}{(4\pi i)^{D/2}} \left(\frac{4}{-\xi_{\mathbf{n}} + i\epsilon} \right)^{(D-2)/4} \frac{1}{(\xi_{\mathbf{n}} - i\epsilon)^{1/2}} \left[s^{D/2} H_{D/2}^{(2)}(s(\xi_{\mathbf{n}} - i\epsilon)^{1/2}) \right]_0^{\sigma}. \quad (2.12)$$

* We should note that our formalism will be easily extended to finite temperature theory. The finite temperature Green function can be obtained by summing the Euclidean Green function so that it has periodicity in the direction of time, in the same way as Eq.(2.9).

The effective potential should take real values physically. The imaginary part of the effective potential must vanish after we take the limit $x \rightarrow x'$. Thus we consider only real part of the effective potential which is given by

$$V = \frac{1}{2\lambda_0}\sigma^2 + \lim_{\mathbf{x}' \rightarrow \mathbf{x}} \text{tr}\mathbf{1} \sum_{\mathbf{n}} \alpha(\mathbf{n}) \frac{1}{(2\pi)^{D/2}} \frac{1}{\Delta x_{\mathbf{n}}^D} \left[(\sigma \Delta x_{\mathbf{n}})^{D/2} K_{D/2}(\sigma \Delta x_{\mathbf{n}}) - \lim_{z \rightarrow 0} z^{D/2} K_{D/2}(z) \right], \quad (2.13)$$

where we have defined

$$\Delta x_{\mathbf{n}} = \sqrt{\sum_{i=1}^{D-1} (x_i - x'_i + n_i L_i)^2}, \quad (2.14)$$

and $K_{\nu}(z)$ is the modified Bessel function. In deriving the above equation, we have set that $t = t'$, and used the relation, $H_{\nu}^{(2)}(-iz) = (i2/\pi)e^{\nu\pi i}K_{\nu}(z)$ (see e.g. [21]).

As is read from Eq.(2.13), only when $\mathbf{n} = 0$ in the summation diverges. We therefore separate the effective potential into two parts,

$$V = V^{\text{IV}} + V^{\text{FV}}, \quad (2.15)$$

where

$$V^{\text{IV}} = \frac{1}{2\lambda_0}\sigma^2 + \lim_{\Delta x \rightarrow 0} \text{tr}\mathbf{1} \frac{1}{(2\pi)^{D/2}} \frac{1}{\Delta x^D} \left[(\sigma \Delta x)^{D/2} K_{D/2}(\sigma \Delta x) - 2^{D/2-1}\Gamma(D/2) \right], \quad (2.16)$$

$$V^{\text{FV}} = \lim_{\mathbf{x}' \rightarrow \mathbf{x}} \text{tr}\mathbf{1} \sum_{\mathbf{n}(\neq 0)} \alpha(\mathbf{n}) \frac{1}{(2\pi)^{D/2}} \frac{1}{\Delta x_{\mathbf{n}}^D} \left[(\sigma \Delta x_{\mathbf{n}})^{D/2} K_{D/2}(\sigma \Delta x_{\mathbf{n}}) - 2^{D/2-1}\Gamma(D/2) \right]. \quad (2.17)$$

Here we have set $\alpha(\mathbf{n} = 0) = 1$, and used that $\lim_{z \rightarrow 0} z^{D/2} K_{D/2}(z) = 2^{D/2-1}\Gamma(D/2)$.

In general, we need to regularize the divergence of V^{IV} by performing the renormalization procedure. It is well known that the divergence can be removed by the renormalization of the coupling constant for $D < 4$. Employing the renormalization condition,

$$\left. \frac{\partial^2 V^{\text{IV}}}{\partial \sigma^2} \right|_{\sigma=\mu} = \frac{\mu^{D-2}}{\lambda_r}, \quad (2.18)$$

we find that Eq.(2.16) reads

$$\begin{aligned} V_{\text{ren}}^{\text{IV}} &= \frac{1}{2\lambda_r}\sigma^2 \mu^{D-2} \\ &+ \lim_{\Delta x \rightarrow 0} \frac{\text{tr}\mathbf{1}}{(2\pi)^{D/2}} \frac{1}{\Delta x^D} \left[\frac{1}{2}(\sigma \Delta x)^2 (\mu \Delta x)^{D/2-1} \left(K_{D/2-1}(\mu \Delta x) - \mu \Delta x K_{D/2-2}(\mu \Delta x) \right) \right. \\ &\quad \left. + (\sigma \Delta x)^{D/2} K_{D/2}(\sigma \Delta x) - 2^{D/2-1}\Gamma(D/2) \right]. \end{aligned} \quad (2.19)$$

As we shall see in the next sections, $V_{\text{ren}}^{\text{IV}}$ reduces to the well known form of the effective potential in the Minkowski spacetime. Therefore the effect of the nontrivial configuration of space on the effective potential is described by V^{FV} .

Finally in this section, we explain the phase factor $\alpha(\mathbf{n})$. As is pointed out in Ref. [22–24] there is no theoretical constraint which boundary condition one should take for quantum fields in compact flat spaces. It is possible to consider the fields with the various boundary condition in the compact spaces with non-trivial topology. Thus we consider the fermion fields with periodic and antiperiodic boundary conditions, and study whether the finite size effect can be changed by the boundary condition. For this purpose, it is convenient to introduce the phase factor $\alpha(\mathbf{n})$ by

$$\alpha(\mathbf{n}) = \alpha_1 \alpha_2 \cdots \alpha_{D-1}, \quad (2.20)$$

where $\alpha_i = (-1)^{n_i}$ for antiperiodic boundary condition in the direction of x_i , and $\alpha_i = 1$ for periodic boundary condition. In the following sections we investigate the behavior of the effective potential at $D = 3$ and $D = 4$ with the various boundary conditions.

III. APPLICATION IN $D = 3$

In this section we apply the method explained in the previous section to the case, $D = 3$. In the three dimensional torus spacetime, $R \otimes S^1 \otimes S^1$, it is possible to consider the three kinds of independent boundary conditions. To see the effect of the compact space and the boundary condition of the field on the phase structure of the four-fermion theory, we evaluate the effective potential and the gap equation and show the phase structure for every three kinds of boundary conditions. As is mentioned before, the same problem has been investigated in Ref. [16] for the three dimensional flat compact space with nontrivial topology. We can compare our results with theirs.

The three dimensional case is instructive because the modified Bessel functions reduce to elementary functions,

$$K_{3/2}(z) = \sqrt{\frac{\pi}{2z}} \left(1 + \frac{1}{z}\right) e^{-z}, \quad (3.1)$$

$$K_{1/2}(z) = K_{-1/2}(z) = \sqrt{\frac{\pi}{2z}} e^{-z}. \quad (3.2)$$

Substituting the relations (3.1) and (3.2) to Eqs.(2.19) and (2.17), the effective potential V in three dimension becomes

$$V = V_{\text{ren}}^{\text{IV}} + V^{\text{FV}}, \quad (3.3)$$

$$\frac{V_{\text{ren}}^{\text{IV}}}{\mu^3} = \frac{1}{2} \left(\frac{1}{\lambda_r} - \frac{\text{tr}\mathbf{1}}{2\pi} \right) \left(\frac{\sigma}{\mu} \right)^2 + \frac{\text{tr}\mathbf{1}}{12\pi} \left(\frac{\sigma}{\mu} \right)^3, \quad (3.4)$$

$$\frac{V^{\text{FV}}}{\mu^3} = \frac{\text{tr}\mathbf{1}}{4\pi} \sum_{\mathbf{n} \neq 0} \frac{\alpha(\mathbf{n})}{(\mu\zeta_{\mathbf{n}})^3} \left(\sigma\zeta_{\mathbf{n}} e^{-\sigma\zeta_{\mathbf{n}}} + e^{-\sigma\zeta_{\mathbf{n}}} - 1 \right), \quad (3.5)$$

where

$$\zeta_{\mathbf{n}} \equiv \lim_{\mathbf{x}' \rightarrow \mathbf{x}} \Delta x_{\mathbf{n}} = \sqrt{(n_1 L_1)^2 + (n_2 L_2)^2}. \quad (3.6)$$

Here we note that Eq.(3.5) disappears in the Minkowski limit $(L_1, L_2) \rightarrow (\infty, \infty)$ and the effective potential (3.3) reduces to Eq.(3.4) which is equal to the effective potential in the Minkowski space-time.

The gap equation, $\partial V / \partial \sigma|_{\sigma=m} = 0$, which determines the dynamical fermion mass m in the compact flat space with nontrivial topology reduces to

$$\frac{4\pi}{\lambda_r \text{tr}\mathbf{1}} - 2 + \frac{m}{\mu} - \sum_{\mathbf{n} \neq 0} \alpha(\mathbf{n}) \frac{e^{-m\zeta_{\mathbf{n}}}}{\mu\zeta_{\mathbf{n}}} = 0. \quad (3.7)$$

The effective potential in the Minkowski spacetime (3.4) has a broken phase in which the discrete chiral symmetry is broken down, when the coupling constant is larger than the critical value $\lambda_{cr} = 2\pi / \text{tr}\mathbf{1}$. For convenience, we introduce the dynamical fermion mass m_0 in the Minkowski space-time given by $\partial V_{\text{ren}}^{\text{IV}} / \partial \sigma|_{\sigma=m_0} = 0$. The dynamical fermion mass m_0 in the Minkowski space-time has a relationship with the coupling constant as

$$\frac{m_0}{\mu} = -\frac{4\pi}{\lambda_r \text{tr}\mathbf{1}} + 2. \quad (3.8)$$

When the system is in the broken phase at the limit of Minkowski space $(L_1, L_2) \rightarrow (\infty, \infty)$, substituting Eq.(3.8) to Eq.(3.7), we obtain the gap equation,

$$\frac{m}{m_0} - 1 - \sum_{\mathbf{n} \neq 0} \alpha(\mathbf{n}) \frac{e^{-m\zeta_{\mathbf{n}}}}{m_0 \zeta_{\mathbf{n}}} = 0. \quad (3.9)$$

It should be noted that the solution m of the gap equation coincides with the dynamical fermion mass $m = m_0$ at the limit $(L_1, L_2) \rightarrow (\infty, \infty)$.

We expect that the phase transition will occur for a sufficiently small L_i . It is convenient to introduce a new variable k_i instead of L_i to investigate the gap equation (3.9) for small L_1 and L_2 .

$$k_i \equiv \left(\frac{2\pi}{L_i} \right)^2. \quad (3.10)$$

To investigate the phase structure of the four-fermion theory in three dimensional flat compact space, we calculate the effective potential (3.3) and the gap equation (3.9) numerically with varying the variable k_i for the various boundary conditions below.

A. Antiperiodic-antiperiodic boundary condition

First we take the antiperiodic boundary condition for both compactified directions and call this case AA-model. The phase factor is chosen as $\alpha(\mathbf{n}) = (-1)^{n_1}(-1)^{n_2}$ in this case. In Fig.1 the behavior of the gap equation (3.9) is shown for the AA-model. As is seen in Fig.1, we find that the symmetry restoration occurs as L_1 and (or) L_2 become smaller and that the phase transition is second-order. In the case of $L_1 = L_2 = L$, the critical value of L where the phase transition takes place is $L_{cr} \approx 1.62/m_0$ ($k_{cr}/m_0^2 \approx 15.1$). In Fig.2 the behavior of the effective potential (3.3) for the AA-model is plotted as a function of σ/μ for the case of $\lambda_r > \lambda_{cr}$ (we take $\lambda_r = 2\lambda_{cr}$ as a typical case). In plotting Figs.1 and 2, we numerically summed \mathbf{n} in Eqs.(3.5) and (3.9). In Fig.3 we show the phase diagram for the AA-model in (L_1, L_2) plane. Here we note that in the limit $L_1 \rightarrow \infty$ (or $L_2 \rightarrow \infty$), the space-time topology $R \otimes S^1 \otimes S^1$, considered here, should be understood as $R^2 \otimes S^1$.

In this limit the field theory should have the same structure as the finite temperature field theory for $D = 3$. In fact, the critical value of L_1 (or L_2) is equal to the critical temperature $\beta_{cr} = 2 \ln 2 \approx 1.39$ as is expected, which is shown by dashed line in the figure. These results consistent with those of Ref. [16] for the model with the A-A boundary condition.

B. Periodic-antiperiodic boundary condition

We consider the case where the periodic and the antiperiodic boundary conditions are adopted in x_1 and x_2 directions, respectively. We call this case PA-model, where the phase is taken as $\alpha(\mathbf{n}) = (-1)^{n_2}$. In Fig.4 we show the behavior of the gap equation (3.9) for the PA-model. From Fig.4, we find that the symmetry restoration occurs when L_2 becomes smaller with L_1 fixed and that the symmetry restoration dose not occur when L_1 becomes smaller with L_2 fixed. We also find that the phase transition is second-order, if occur. Especially in the case of $L_1 = L_2 = L$, the symmetry restoration occur, and the critical value L_{cr} where the symmetry is restored is $m_0 L_{cr} \approx 1.14$ ($k_{cr}/m_0^2 \approx 30.3$). In Figs.5, 6 and 7 typical behaviors of the effective potential for the PA-model are shown as a function of σ/μ for the case of $\lambda_r > \lambda_{cr}$ (we take $\lambda_r = 2\lambda_{cr}$). Fig.5 is the case of $L_1 = L_2$. Fig.6 is the case with L_1 fixed, and Fig.7 is same but with L_2 fixed. In Fig.6, where L_1 (the size associated with the periodic boundary condition) is fixed, we can see that the chiral symmetry is restored as L_2 (the size associated with the anti-priodic boundary condition) becomes smaller. While, in Fig.7 where L_2 is fixed, the fermion mass becomes larger as L_1 becomes smaller. The phase diagram for the PA-model is shown in Fig.8 in (L_1, L_2) plane. These results is consistent with those of Ref. [16].

C. Periodic-periodic boundary condition

Finally we take the periodic boundary condition for both compactified directions and call this case PP-model. The phase factor is chosen as $\alpha(\mathbf{n}) = 1$ in this case. In Fig.9, we show the behavior of the gap equation (3.9) for the PP-model. From this figure, we find

that the symmetry restoration does not occur as L_1 and (or) L_2 becomes smaller. In Fig.10, we show the effective potential (3.3) in the case of $L_1 = L_2 = L$ and $\lambda_r > \lambda_{cr}$ (we take $\lambda_r = 2\lambda_{cr}$) for the PP-model.

Especially, in the case of $L_1 = L_2 = L$, we can analytically prove that the symmetry restoration doesn't occur irrespective of the coupling constant λ_r . To see this, we investigate the differential coefficient of the effective potential (3.3) of the PP-model at $\sigma \rightarrow 0+$. The differential coefficient of the effective potential (3.3) is

$$\frac{1}{\mu^2} \frac{dV}{d\sigma} = \frac{\sigma}{\mu} \left(\frac{1}{\lambda_r} - \frac{\text{tr}\mathbf{1}}{2\pi} + \frac{\text{tr}\mathbf{1}}{4\pi} \frac{\sigma}{\mu} - \frac{\text{tr}\mathbf{1}}{4\pi} \sum_{\mathbf{n} \neq 0} \frac{e^{-\sigma\zeta_{\mathbf{n}}}}{\mu\zeta_{\mathbf{n}}} \right). \quad (3.11)$$

Taking the limit $\sigma \rightarrow 0+$, Eq.(3.11) reduces to

$$\left. \frac{1}{\mu^2} \frac{dV}{d\sigma} \right|_{\sigma \rightarrow 0+} = - \frac{\text{tr}\mathbf{1}\sigma}{\mu\pi} \sum_{n_1=1}^{\infty} \sum_{n_2=1}^{\infty} \frac{e^{-\sigma L \sqrt{n_1^2 + n_2^2}}}{\mu L \sqrt{n_1^2 + n_2^2}} \Big|_{\sigma \rightarrow 0+}. \quad (3.12)$$

Using an inequality,

$$\frac{n_1 + n_2}{\sqrt{2}} \leq \sqrt{n_1^2 + n_2^2} < n_1 + n_2, \text{ for } n_1 \geq 1 \text{ and } n_2 \geq 1, \quad (3.13)$$

we get the inequality

$$\frac{e^{-\sigma L(n_1+n_2)}}{n_1 + n_2} < \frac{e^{-\sigma L \sqrt{n_1^2 + n_2^2}}}{\sqrt{n_1^2 + n_2^2}} \leq \frac{\sqrt{2} e^{-\sigma L(n_1+n_2)/\sqrt{2}}}{n_1 + n_2}. \quad (3.14)$$

Summing up each term in Eq.(3.14) with respect to n_1 and n_2 , we find,

$$\frac{1}{e^{\sigma L} - 1} + \log(1 - e^{-\sigma L}) < \sum_{n_1=1}^{\infty} \sum_{n_2=1}^{\infty} \frac{e^{-\sigma L \sqrt{n_1^2 + n_2^2}}}{\sqrt{n_1^2 + n_2^2}} \leq \frac{\sqrt{2}}{e^{\sigma L/\sqrt{2}} - 1} + \sqrt{2} \log(1 - e^{-\sigma L/\sqrt{2}}). \quad (3.15)$$

According to Eq.(3.15), we obtain the inequality

$$\left. \frac{1}{\mu^2} \frac{dV}{d\sigma} \right|_{\sigma \rightarrow 0+} < - \frac{\text{tr}\mathbf{1}\sigma}{\pi\mu^2 L} \left(\frac{1}{e^{\sigma L} - 1} + \log(1 - e^{-\sigma L}) \right) \Big|_{\sigma \rightarrow 0+} = - \frac{\text{tr}\mathbf{1}}{\pi\mu^2 L^2} < 0. \quad (3.16)$$

We find that the differential coefficient of the effective potential has a negative value at $\sigma \rightarrow 0+$ irrespective of the coupling constant λ_r in the case of $L_1 = L_2 = L$ for the PP-model.

Thus, we have shown that only a broken phase could exist and the symmetry restoration does not occur at all. Though this proof is limited to the special case $L_1 = L_2 = L$, this result is expected to hold in other cases $L_1 \neq L_2$. The results in this subsection are different from those of Ref. [16] for PP-model.

Summarizing this section, we examined the phase structure of the four-fermion theory in compactified space of the three dimension by evaluating the effective potential. The phase structure is altered due to the compactified space. Our results are consistent with those of Ref. [16] except for the periodic-periodic boundary condition. In the case of PP-model, our results indicate that only a broken phase could exist and the symmetry restoration dose not occur.

The behavior of the dynamical fermion mass m is quite different according as the imposed boundary condition. Making the length size of the compactified direction small, the dynamical fermion mass becomes large when adopting the periodic boundary condition. However it becomes small when adopting the antiperiodic boundary condition. In concrete, for the AA-model where the antiperiodic boundary condition is imposed in the two directions, the dynamical fermion mass disappears, and the symmetry is restored when the size of the compactified space becomes small. The order of the symmetry restoration is second. In the PP-model, where the periodic boundary condition is imposed, the symmetry is not restored as is seen before. In the PA-model, where one direction is periodic boundary condition and the other is antiperiodic one, two effects compete with each other. In the special case $L_1 = L_2 = L$ the effect of antiperiodic boundary condition triumphs over that of periodic boundary condition to restore the symmetry at small L . The order of this symmetry restoration is second.

IV. APPLICATION IN $D = 4$

In this section we consider the case of $D = 4$, i.e., the spacetime which has 3-dimensional spatial sector with nontrivial topology. Let us start evaluating $V_{\text{ren}}^{\text{IV}}$. The special situation

in $D = 4$ case is that the renormalization can not make finite the effective potential in our theory. Therefore it is not necessary to consider the renormalization for $D = 4$. Nevertheless, we introduce a "renormalized" coupling constant defined by Eq.(2.19) for convenience in the same way as the case in $D = 3$.

Then we must regularize $V_{\text{ren}}^{\text{IV}}$ by some method, e.g., by introducing a cut-off parameter. Here we examine two methods to regularize $V_{\text{ren}}^{\text{IV}}$. The first one is to keep Δx finite and to set $D = 4$. The straightforward calculations lead to

$$\begin{aligned} \frac{V_{\text{ren}}^{\text{IV}}}{\mu^4} &= \frac{1}{2\lambda_r} \left(\frac{\sigma}{\mu}\right)^2 + \frac{\text{tr}\mathbf{1}}{4(4\pi)^2} \left[\left(\frac{\sigma}{\mu}\right)^2 \left(-2 + 12\left(\gamma - \ln \frac{2}{\mu\Delta x}\right)\right) \right. \\ &\quad \left. + \left(\frac{\sigma}{\mu}\right)^4 \left(\frac{3}{2} - 2\left(\gamma - \ln \frac{2}{\mu\Delta x} + \ln \frac{\sigma}{\mu}\right)\right) \right] + O(\Delta x), \end{aligned} \quad (4.1)$$

from Eq.(2.19). On the other hand one can adopt the dimensional regularization as the second method, in which we set $D = 4 - 2\epsilon$. By expanding the right hand side of Eq.(2.19) in terms of $1/\epsilon$, we find

$$\begin{aligned} \frac{V_{\text{ren}}^{\text{IV}}}{\mu^D} &= \frac{1}{2\lambda_r} \left(\frac{\sigma}{\mu}\right)^2 + \frac{\text{tr}\mathbf{1}}{4(4\pi)^2} \left[\left(\frac{\sigma}{\mu}\right)^2 \left(-2 + 6\left(\gamma - \ln 4\pi\right) - \frac{6}{\epsilon}\right) \right. \\ &\quad \left. + \left(\frac{\sigma}{\mu}\right)^4 \left(\frac{3}{2} - \left(\gamma - \ln 4\pi + 2 \ln \frac{\sigma}{\mu}\right) + \frac{1}{\epsilon}\right) \right] + O(\epsilon). \end{aligned} \quad (4.2)$$

The above two methods are related by

$$\frac{1}{\epsilon} = -\gamma + \ln\left(\frac{1}{(\mu\Delta x)^2\pi}\right). \quad (4.3)$$

According to the Ref. [4,2], we find the momentum cut-off parameter Λ , which is introduced in their papers, is related by

$$\ln \frac{\Lambda^2}{\mu^2} = \ln\left(\frac{2}{\mu\Delta x}\right)^2 + 1 - 2\gamma. \quad (4.4)$$

This effective potential has a broken phase, when the coupling constant is larger than the critical value λ_{cr} , which is given by

$$\frac{1}{\lambda_{\text{cr}}} = \frac{\text{tr}\mathbf{1}}{(4\pi)^2} \left(3 \ln \frac{\Lambda^2}{\mu^2} - 2\right). \quad (4.5)$$

For convenience, we introduce the dynamical fermion mass m_0 in the Minkowski space by

$$\frac{1}{\lambda_r} - \frac{1}{\lambda_{cr}} + \frac{\text{tr}\mathbf{1}}{(4\pi)^2} \left(\ln \frac{\Lambda^2}{m_0^2} \right) \frac{m_0^2}{\mu^2} = 0, \quad (4.6)$$

as in the case in $D = 3$. In terms of m_0 , Eq.(4.1) or Eq.(4.2) can be written as

$$\frac{V_{\text{ren}}^{\text{IV}}}{m_0^4} = \frac{\text{tr}\mathbf{1}}{4(4\pi)^2} \left[-2 \left(\ln \frac{\Lambda^2}{m_0^2} \right) \frac{\sigma^2}{m_0^2} + \left(\ln \frac{\Lambda^2}{m_0^2} + \frac{1}{2} - \ln \frac{\sigma^2}{m_0^2} \right) \frac{\sigma^4}{m_0^4} \right], \quad (4.7)$$

where we used the momentum cut-off parameter.

On the other hand, Eq.(2.17), which represents the effect due to the compactified space, reduces to

$$\frac{V^{\text{FV}}}{m_0^4} = \frac{\text{tr}\mathbf{1}}{(2\pi)^2} \sum_{\mathbf{n} \neq 0} \frac{\alpha(\mathbf{n})}{(m_0 \zeta_{\mathbf{n}})^4} \left[(\sigma \zeta_{\mathbf{n}})^2 K_2(\sigma \zeta_{\mathbf{n}}) - 2 \right], \quad (4.8)$$

where $\zeta_{\mathbf{n}} = \sqrt{(n_1 L_1)^2 + (n_2 L_2)^2 + (n_3 L_3)^2}$.

Then we get the gap equation

$$-\ln \frac{\Lambda^2}{m_0^2} + \frac{m^2}{m_0^2} \left(\ln \frac{\Lambda^2}{m_0^2} - \ln \frac{m^2}{m_0^2} \right) - 4 \sum_{\mathbf{n} \neq 0} \frac{\alpha(\mathbf{n})}{(m_0 \zeta_{\mathbf{n}})} \frac{m}{m_0} K_1(m \zeta_{\mathbf{n}}) = 0. \quad (4.9)$$

We can easily solve the above equation numerically. The advantage of our method is that the equation is given by a simple sum of the modified Bessel function which damps exponentially at large \mathbf{n} .

In $D = 4$ case, we have many varieties of models according to the varieties of the size of torus and the boundary condition of fermion fields in the three different directions of torus. For convenience, we separate this section into the following three subsections.

A. Antiperiodic boundary conditions

Let us first consider the models associated with the antiperiodic boundary condition for fermion fields, where the phase parameter is given by $\alpha(\mathbf{n}) = (-1)^{n_1} (-1)^{n_2} (-1)^{n_3}$. In Fig.11 we show the behavior of solutions of the gap equation with the antiperiodic boundary condition on the three typical spaces with non-trivial topology. That is, one is the torus of three equal sides ($L_1 = L_2 = L_3 = L$), which we call this case AAA-model, second is the torus but with a infinite side, i.e., ($L_1 = L_2 = L, L_3 = \infty$), AAI-model, third is the

space with only one side compactified ($L_1 = L, L_2 = L_3 = \infty$), which we call AII-model. The three lines in the figure show the solution of the gap equations on the three spaces as the function of $(2\pi/Lm_0)^2$. For a direction x_i with a infinite side, the sum of n_i becomes ineffective. Here we have taken the cut-off parameter $\Lambda/m_0 = 10$.[†]

In Fig.11 we have considered the models which have broken phase for large L . The figure shows that the symmetric phase appears as L become smaller beyond some critical values. Thus as is expected from the results of $D = 3$, the effect of compactifying the space affects the phase structure, and the effect with the antiperiodic boundary condition for fermion fields always tends to restore the symmetry.

We show the critical values L_{cr} , i.e., the value of L when the symmetry is restored, as a function of cut-off parameter in Fig.12. We can read from the figure that smaller value of L is needed in order to restore the symmetry of the AII-model compared with AAA-model .

B. Periodic boundary conditions

Next we consider the fields with the periodic boundary condition, where the phase parameter is taken as $\alpha(\mathbf{n}) = (+1)^{n_1} (+1)^{n_2} (+1)^{n_3}$. In the same way as the above, consider three typical kinds of spaces, ($L_1 = L_2 = L_3 = L$), ($L_1 = L_2 = L, L_3 = \infty$), and ($L_1 = L, L_2 = L_3 = \infty$), with adopting the periodic boundary condition for the compactified directions. We call each of them PPP-, PPI-, PII-model, respectively. The solutions of gap equation are shown in Fig.13. In contrast to the results of antiperiodic boundary condition, the fermion mass of broken phase becomes larger as L becomes smaller. The effect becomes more significant as the scale of compactification L becomes smaller. This nature is same as the results in $D = 3$.

Fig.13 shows the case that the coupling constant is larger than the critical value of

[†] In the below, the cut-off parameter $\Lambda/m_0 = 10$ is adopted tacitly, as long as we do not note especially.

Minkowski spacetime, i.e., $\lambda_r > \lambda_{cr}$, and that the phase is broken in the limit $L \rightarrow \infty$. The phase structure of these fields with the periodic boundary condition has the interesting feature that the phase becomes broken due to the compactified space even when the coupling constant is smaller than the critical value and the phase is symmetric in the limit of $L \rightarrow \infty$. In order to show this, let us introduce a “mass” m_1 instead of the coupling constant by

$$\left| \frac{1}{\lambda_r} - \frac{1}{\lambda_{cr}} \right| + \frac{\text{tr}\mathbf{1}}{(4\pi)^2} \left(\ln \frac{\Lambda^2}{m_1^2} \right) \frac{m_1^2}{\mu^2} = 0. \quad (4.10)$$

Then the gap equation reduces to

$$\ln \frac{\Lambda^2}{m_1^2} + \frac{m^2}{m_1^2} \left(\ln \frac{\Lambda^2}{m_1^2} - \ln \frac{m^2}{m_1^2} \right) - 4 \sum_{\mathbf{n} \neq 0} \frac{\alpha(\mathbf{n})}{(m_1 \zeta_{\mathbf{n}})} \frac{m}{m_1} K_1(m \zeta_{\mathbf{n}}) = 0. \quad (4.11)$$

We show the solution of the gap equation in Fig.14. Here the cut-off parameter is chosen as $\Lambda/m_1 = 10$. The fermion mass becomes non-zero value and the broken phase appears as L becomes smaller in the compactified spaces. Thus the effect of compactified space makes the phase broken when the periodic boundary condition is considered.

C. Antiperiodic and periodic boundary conditions

The above investigation suggests that the dynamical phase of the fields is significantly affected by the compactification of the spatial sector. The effect works in different way according to the boundary conditions of the fermion fields. In this subsection, we consider the models in which the different boundary conditions are adopted for different directions of compact space, to check these features in more detail.

First we consider the model that the periodic boundary condition is imposed in the x_1 -direction in the period $L_1 = L_P$ and the antiperiodic boundary condition in the x_2 -direction in the period $L_2 = L_A$ and the other side is infinite, i.e., $L_3 = \infty$. We call this case PAI-model. Fig.15 shows the phase diagram of the PAI-model, which has the broken phase in the limit of Minkowski space, in the $(L_P - L_A)$ plane. The critical value of L_A at large L_P is $m_0 L_A \simeq 1.20$. We find the similar behavior in section 3-B. We next consider the model that

the periodic boundary condition is imposed in the x_1 -direction in the period $L_1 = L_P$ and the antiperiodic boundary condition in the x_2 - and x_3 -direction in the period $L_2 = L_3 = L_A$, which we call this PAA-model. Fig.16 is the phase diagram of PAA-model in the $(L_P - L_A)$ plane. The critical value of L_A at large L_P is $m_0 L_A \simeq 1.38$. Finally we consider the PPA-model, i.e., the periodic boundary condition is imposed in the x_1 - and x_2 -direction in the period $L_1 = L_2 = L_P$ and the antiperiodic boundary condition in the x_3 -direction in the period $L_3 = L_A$. Fig.17 is the phase diagram of PPA-model. The critical value of L_A at large L_P is same as that of PAI-model. All these models show the similar behavior in the subsection 3-B.

To end this section, we summarize the results. We have investigated the nature of the effective potential in the compactified space in four dimension. The effect of the compactification of the spatial sector changes the phase structure of the four-fermion theory. The consequent results on the effective potential comes up in different way according to the boundary condition of the fermion fields. The antiperiodic boundary condition tends to restore the symmetry and the periodic boundary condition does to break the symmetry, when the effect of the compact space becomes large. Thus we can construct the both models that the symmetry is broken and restored in the course of the expansion of the universe.

V. SUMMARY AND DISCUSSIONS

We have investigated the four-fermion theory in compact flat space with non-trivial topology. By using the effective potential and the gap equation in the leading order of the $1/N$ expansion we find the phase structure of the theory in three and four spacetime dimensions. In three dimensions three class of models are considered according to the variety of the boundary conditions for fermion fields. The phase structure of the theory is examined for three models. When taking the antiperiodic boundary condition, the broken chiral symmetry tends to be restored for a sufficiently small L . The phase transition is of the second order. When taking the periodic boundary condition, the chiral symmetry tends

to be broken down for a small L . In four dimensions we also see the same effects appears in the compact flat spaces.

Therefore the drastic change of the phase structure is induced by the compact space with no curvature. In the torus space with the antiperiodic boundary condition, the finite size effect decreases the dynamical fermion mass and the chiral symmetry is restored for a small universe beyond some critical size ($L < L_{cr}$). On the other hand, the torus space with the periodic boundary condition for fermion fields, the finite size effect causes the opposite influence to the phase structure. The dynamical fermion mass is increased as the size L decreases and the chiral symmetry may be broken down for $L < L_{cr}$, even when we set symmetric phase at $L \rightarrow \infty$. In some cases only the broken phase is observed for any finite L ($L_{cr} \rightarrow \infty$) even if the coupling constant λ_r of the four-fermion interactions is sufficiently small.

According to the behavior of the effective potential in section 3, the value of the vacuum energy in the true vacuum becomes lower when the space size (volume) of the compactified direction becomes small in the model associated with the periodic boundary condition. On the contrary, for the model associated with the the antiperiodic boundary condition, the value of the the vacuum energy in the true vacuum is raised, when the space size (volume) becomes small. Therefore we find that the effect of the periodic boundary condition forces attractively (negative pressure) and that of antiperiodic boundary condition forces repulsively (positive pressure). This fact resembles to the well known Casimir effect [25], which is found in QED. The Casimir effect gives rise to the vacuum pressure due to the effect of the finite volume.

Using the momentum space representation we understand these effects of boundary conditions in the following way. In the compactified space the momentum is discretized. The fermion fields with an antiperiodic boundary condition can not take a momentum smaller than ($|p| \geq \pi/L$). Thus the possible momentum of the internal fermion fields becomes larger when L becomes small. Since the lower momentum fermion field has played an essential role to break the chiral symmetry, the vacuum expectation value of the composite operator $\langle \bar{\psi}\psi \rangle$

disappears for a sufficiently small L and the broken symmetry is restored. Contrary to this the fermion fields with a periodic boundary condition can take a vanishing momentum even if the space is compact. Hence the finite size of L has no effect to restore the symmetry. In the compactified space the fermion field $\psi(x)$ can interact with the field $\psi(x + nL)$ for a compactified direction. Thus the finite size effect seems to make the interaction stronger. Summing up all the correlations $\langle \bar{\psi}(x)\psi(x + nL) \rangle$, the vacuum expectation value of the composite field becomes larger as L decreases. We can understand it as the dimensional reduction. Compactifying one direction to the size L in D -dimensional space, it looks $D - 1$ -dimensional space for particles with Compton wavelength much larger than the size L . In the lower dimensional space the influence from the lower momentum fermion exceeds. Then the finite size effect breaks the chiral symmetry for the model with the periodic boundary condition.

From the cosmological point of view, some mechanism, e.g., inflation, is needed to explain the hot and large universe. Even in the torus universe, inflation seems to be needed to solve the horizon problem. As had been discussed in Ref. [26], we need some special idea to lead inflation in the context of the dynamical symmetry breaking scenario. An inflation model which is induced by a composite fermion field in the context of the dynamical symmetry breaking scenario is investigated in some class of supersymmetric particle model [27]. We will need further investigation to test the symmetry breaking in the early universe.

ACKNOWLEDGMENTS

We would like to thank professor T. Muta for useful discussions and comments. We also thanks M. Siino for helpful comments.

APPENDIX:

In the present paper we have calculated the effective potential starting from the Feynman propagator defined by Eq.(2.9). The spacetime considered here reduces to the cylindrical

universe $R \otimes S^1$ for $D = 2$. The effective potential of the four-fermion theory in a cylindrical universe can be obtained by using another representation of the Feynman propagator. [17,9] To justify our method we calculate the effective potential (2.15) in two dimensions and compare it with the result given in Ref. [9].

Taking the two dimensional limit Eqs.(2.19) and (2.17) read

$$V_{\text{ren}}^{\text{IV}} = \frac{1}{2} \left(\frac{1}{\lambda_r} - \frac{3\text{tr}\mathbf{1}}{4\pi} \right) \sigma^2 + \frac{\text{tr}\mathbf{1}}{8\pi} \sigma^2 \ln \left(\frac{\sigma}{\mu} \right)^2, \quad (\text{A1})$$

$$V^{\text{FV}} = \sum_{n=1}^{\infty} \alpha(n) \frac{\text{tr}\mathbf{1}}{\pi n L} |\sigma| \left[K_1(|\sigma|nL) - \frac{1}{|\sigma|nL} \right], \quad (\text{A2})$$

respectively. Eq.(A1) is exactly equal to the effective potential of Gross-Neveu model in two-dimensional Minkowski space. Thus the other part of the effective potential V^{FV} gives the finite size and topological effect also in $R \otimes S^1$. To compare the results with the one obtained by another method we change the expression of V^{FV} .

The effective potential V^{FV} can be written as

$$V^{\text{FV}} = -\frac{\text{tr}\mathbf{1}}{\pi} \int_0^\sigma s ds \sum_{n=1}^{\infty} \alpha(n) K_0(n|s|L). \quad (\text{A3})$$

Now we use the formula

$$\begin{aligned} I(x) &= \sum_{n=1}^{\infty} \alpha(n) K_0(nx), \\ &= \sum_{n=1}^{\infty} \alpha(n) \int_0^\infty dt \frac{\cos(nxt)}{\sqrt{t^2 + 1}}, \\ &= \int_0^\infty dt \frac{1}{2\sqrt{t^2 + 1}} \left(\sum_{n=-\infty}^{\infty} e^{in\beta(xt)} - 1 \right), \end{aligned} \quad (\text{A4})$$

where the variable $\beta(xt)$ depends on the boundary condition and given by

$$\beta(xt) = \begin{cases} xt, & \text{periodic boundary condition,} \\ xt + \pi, & \text{antiperiodic boundary condition.} \end{cases} \quad (\text{A5})$$

Performing the summation in Eq.(A4), the function $I(x)$ reads

$$I(x) = \int_0^\infty d\omega \frac{1}{\sqrt{\omega^2 + x^2}} \left(\pi \delta_p(\beta(\omega)) - \frac{1}{2} \right), \quad (\text{A6})$$

where $\delta_p(x)$ is the periodic delta function defined by

$$\delta_p(x) = \frac{1}{2\pi} \sum_{n=-\infty}^{\infty} e^{inx}. \quad (\text{A7})$$

To obtain (A6) we change the integration variable t to $\omega = xt$. According to the property of $\delta_p(x)$ Eq.(A6) can be represented in the following form

$$I(x) = \sum_{n=0}^{\infty} \frac{\pi}{\sqrt{\omega_n^2 + x^2}} - \frac{1}{2} \int_0^{\infty} d\omega \frac{1}{\sqrt{\omega^2 + x^2}}, \quad (\text{A8})$$

where ω_n is given by

$$\omega_n = \begin{cases} 2n\pi, & \text{periodic boundary condition,} \\ (2n+1)\pi, & \text{antiperiodic boundary condition.} \end{cases} \quad (\text{A9})$$

Substituting Eq.(A8) to Eq.(A3), the integrand of the Eq.(A3) is modified as

$$V^{\text{FV}} = -\frac{\text{tr}\mathbf{1}}{\pi} \int_0^{\sigma} s \, ds \left[\frac{\pi}{L} \sum_{n=0}^{\infty} \frac{1}{\sqrt{(\omega_n/L)^2 + s^2}} - \frac{1}{2} \int_0^{\infty} d\omega \frac{1}{\sqrt{(\omega/L)^2 + s^2}} \right]. \quad (\text{A10})$$

We can easily perform the integration over s and find

$$V^{\text{FV}} = -\frac{\text{tr}\mathbf{1}}{L} \sum_{n=0}^{\infty} \left(\sqrt{\left(\frac{\omega_n}{L}\right)^2 + \sigma^2} - \left|\frac{\omega_n}{L}\right| \right) + \frac{\text{tr}\mathbf{1}}{2\pi} \int_0^{\infty} d\omega \left(\sqrt{\left(\frac{\omega}{L}\right)^2 + \sigma^2} - \left|\frac{\omega}{L}\right| \right). \quad (\text{A11})$$

Using the momentum space representation of the Feynman propagator the effective potential of the Gross-Neveu model is given by

$$V^{\text{IV}} = \frac{1}{2\lambda_0} \sigma^2 - \text{tr}\mathbf{1} \int_0^{\infty} \frac{dk}{2\pi} \left(\sqrt{k^2 + \sigma^2} - |k| \right), \quad (\text{A12})$$

in two-dimensional Minkowski spacetime. Inserting Eqs.(A11) and (A12) into Eq.(2.15) the effective potential in $R \otimes S^1$ reads

$$V = \frac{1}{2\lambda_0} \sigma^2 - \frac{\text{tr}\mathbf{1}}{L} \sum_{n=0}^{\infty} \left(\sqrt{\left(\frac{\omega_n}{L}\right)^2 + \sigma^2} - \left|\frac{\omega_n}{L}\right| \right). \quad (\text{A13})$$

In the case of the antiperiodic boundary condition Eq.(A13) reproduces the result obtained in Ref. [17,9]. It is well-known that the field theory in $R \otimes S^1$ is equivalent to the

finite-temperature field theory [‡]. As is shown in Ref. [9], the effective potential (A13) is in agreement with that of the finite temperature four-fermion theory in $D = 2$ with recourse to the relation between the size of the universe L and the temperature T

$$L = \frac{1}{k_B T} \quad (\text{A14})$$

with k_B the Boltzmann constant. In this case it is known that the broken chiral symmetry is restored for sufficiently small $L < L_{cr}$ at the large N limit. The critical size of the universe is given by

$$L_{cr} m_0 = \pi e^{-\gamma}, \quad (\text{A15})$$

where γ is the Euler constant. It is equal to the well-known formula of the critical temperature for the Gross-Neveu model at finite temperature [28].

On the other hand the symmetric phase is not observed for any values of the coupling constant λ_r and L in the case of the periodic boundary condition as is shown below. Using the Eqs. (A1) and (A11), the gap equation of the present theory is given by

$$\frac{dV}{d\sigma} = \sigma \left[\frac{1}{\lambda_r} - \frac{\text{tr}\mathbf{1}}{4\pi} \left(2 - \ln \left| \frac{\sigma}{\mu} \right|^2 \right) - \sum_{n=0}^{\infty} \frac{\text{tr}\mathbf{1}}{\sqrt{\omega_n^2 + (L\sigma)^2}} - \frac{\text{tr}\mathbf{1}}{2\pi} \int_0^{\infty} d\omega \frac{1}{\sqrt{(\omega/L)^2 + \sigma^2}} \right] = 0. \quad (\text{A16})$$

If we take the limit, $\sigma \rightarrow +0$, we find that

$$\left. \frac{dV}{d\sigma} \right|_{\sigma \rightarrow +0} \rightarrow -\frac{1}{L}. \quad (\text{A17})$$

The derivative of the effective potential has a negative value at $\sigma \rightarrow +0$. Thus the minimum of the effective potential is located at non-vanishing σ and the chiral symmetry is always broken down for the fermion field with periodic boundary condition irrespective of the value of the coupling constant λ_r . Evaluating the effective potential numerically we see that the

[‡]In the finite temperature field theory it is forbidden to choose the periodic boundary condition for a fermion field

dynamically generated fermion mass becomes heavier as the size L decreased. Therefore the boundary condition change the finite size effect conversely also in two dimensions and our method agrees with the well-known results.

REFERENCES

- [1] Y.Nambu and G.Jona-Lasinio, Phys. Rev. **122**, 345 (1961).
- [2] T.Inagaki, T.Muta, S.D.Odintsov. Mod. Phys. Lett.**A8**, 2117 (1993).
- [3] E.Elizalde, S.Leseduarte, S.D.Odintsov and Yu.I.Shil'nov, Phys. Rev. **D53**, 1917 (1996).
- [4] T.Inagaki, preprint HUPD-9522 1995.
- [5] E.Elizalde, S.Leseduarte and S.D.Odintsov, Phys. Rev. **D49**, 5551 (1994).
- [6] E.Elizalde, S.Leseduarte and S.D.Odintsov, Phys. Lett. **B347**, 33 (1995);
B.Geyer and S.D.Odintsov, hep-th/9602110 and 9603172.
- [7] T.Inagaki, S. Mukaigawa, and T.Muta, Phys. Rev. **D52**, 4267 (1995).
- [8] E.Elizalde, S.D.Odintsov and Yu.I.Shil'nov, Mod. Phys. Lett. **A9**, 913 (1994).
- [9] K.Ishikawa, T.Inagaki, T.Muta, Mod.Phys.Lett. **A11**, 939 (1996).
- [10] Ya.B.Zeldovich, Comm. Astrophys. Space Phys. **5**, 169 (1973).
- [11] D.D.Sokoloff and V.F.Shvartsman, Sov. Phys. JETP **39** 196 (1974).
- [12] L.Z.Fang and H. Sato, Comm. Theor. Phys. **2**, 1055 (1983).
- [13] I. Yu. Sokolov, Sov. Phys. JETP Lett. **57**, 617 (1993); A. A. Starobinsky, Sov. Phys. JETP Lett. **57**, 622 (1993); A. de Oliveira-Costa and G.F.Smoot, Astrophys. J. **448**, 477 (1995); N.J. Cornish, D.N.Spergel, and G.D.Starkman, preprint, gr-qc/9602039.
- [14] G.F.Smoot, et al., Astrophys. J. **396**, L1 (1992).
- [15] D.Atkatz, and H. Pagels, Phys. Rev. **D25**, 2065 (1982).
- [16] D.K.Kim, Y.D.Han, and I.G.Koh, Phys. Rev. **D 49**, 6943 (1994).
- [17] S.K.Kim, W.Namgung, K.S.Soh and J.H.Yee, Phys. Rev. **D36**, 3172 (1987).

- [18] D.Y.Song, Phys. Rev.**D48**, 3925 (1993).
- [19] D.J.Gross and A. Neveu, Phys. Rev. **D10**, 3235 (1974).
- [20] N. D. Birrell and P. C. W. Davies, *Quantum field theory in curved spacetime*, (Cambridge University Press, Cambridge, 1982).
- [21] W. Magnus, F. Oberhettinger and R. P. Soni, *Formulas and Theorems for the Special Functions of Mathematical Physics*, (Springer-Verlag, Berlin, 1966).
- [22] C.J.Isham, Proc. R. Lond. A.**362**, 383 (1978).
- [23] J.S.Dowker and R.Banach, J. Phys. **A11**, 2255 (1978).
- [24] S.J.Avis and C.J.Isham, Nucl. Phys. **B156**, 441 (1979).
- [25] H.G.B.Casimir, Proc. K. Ned. Akad. wet. **51**, 793 (1948).
- [26] A.M.Matheson, R.D.Ball, A.C.Davis, and R.H.Brandenberger, Nucl. Phys. **B328**, 223 (1989).
- [27] M.Cvtic, T.Hubsch, J.C.Pati, and H.Stremnitzer, Phys. Rev. **D40**, 1311 (1989).
- [28] H.O.Wada, Lett. Nuovo Cim. **11**, 697 (1974);
L.Jacobs, Phys. Rev. **D10**, 3956 (1974);
R.F.Dashen, S.Ma and R.Rajaraman, Phys. Rev. **D11**, 1499 (1975);
D.J.Harrington and A.Yildiz, Phys. Rev. **D11**, 779 (1975);
W.Dittrich and B.G.Englert, Nucl. Phys. **B179**, 85 (1981);
T.Inagaki, T.Kouno, and T.Muta, Int. J. Mod. Phys **A10**, 2241 (1995).

Figure Captions

Fig. 1 Solution of the gap equation for the AA-model.

Fig. 2 Behavior of the effective potential for the AA-model in the case of $L_1 = L_2 = L$. We have set $\lambda_r = 2\lambda_{cr}$, and used the notation $\hat{k} \equiv k/\mu^2$, $\hat{\sigma} \equiv \sigma/\mu$, $\hat{V} \equiv V/(\text{tr}\mathbf{1}\mu^3)$. The critical value is $k_{cr}/m_0^2 \approx 15.1$.

Fig. 3 The phase diagram for the AA-model.

Fig. 4 Solution of the gap equation for the PA-model.

Fig. 5 Behavior of the effective potential for the PA-model in the case of $L_1 = L_2 = L$. Here we have set $\lambda_r = 2\lambda_{cr}$, $\hat{k} \equiv k/\mu^2$, $\hat{\sigma} \equiv \sigma/\mu$, $\hat{V} \equiv V/(\text{tr}\mathbf{1}\mu^3)$. The critical value is $k_{cr}/m_0^2 \approx 30.3$.

Fig. 6 Behavior of the effective potential for the PA-model with L_1 fixed by $\hat{k}_1 = 10.0$. Here we have set $\lambda_r = 2\lambda_{cr}$, $\hat{k}_i \equiv k_i/\mu^2$, $\hat{\sigma} \equiv \sigma/\mu$, $\hat{V} \equiv V/(\text{tr}\mathbf{1}\mu^3)$. The critical value is $k_{2cr}/m_0^2 \approx 21.9$.

Fig. 7 Behavior of the effective potential for the PA-model with L_2 fixed by $\hat{k}_2 = 10.0$. Here we have set $\lambda_r = 2\lambda_{cr}$, $\hat{k}_i \equiv k_i/\mu^2$, $\hat{\sigma} \equiv \sigma/\mu$, $\hat{V} \equiv V/(\text{tr}\mathbf{1}\mu^3)$.

Fig. 8 The phase diagram for the PA-model.

Fig. 9 Behavior of the gap equation for the PP-model.

Fig. 10 Behavior of the effective potential for the PP-model in the case of $L_1 = L_2 = L$.
The notations are same as Fig.(5).

Fig. 11 Solution of the gap equation for the models with antiperiodic boundary condition.

Fig. 12 The cut-off dependence of the critical value of $(2\pi/L_{\text{cr}}m_0)^2$.

Fig. 13 Solution of the gap equation for the models with periodic boundary condition.

Fig. 14 fermion mass of the models with $\lambda_r < \lambda_{\text{cr}}$.

Fig. 15 The phase diagram for the PAI-model.

Fig. 16 The phase diagram for the PAA-model.

Fig. 17 The phase diagram for the PPA-model.

FIGURES

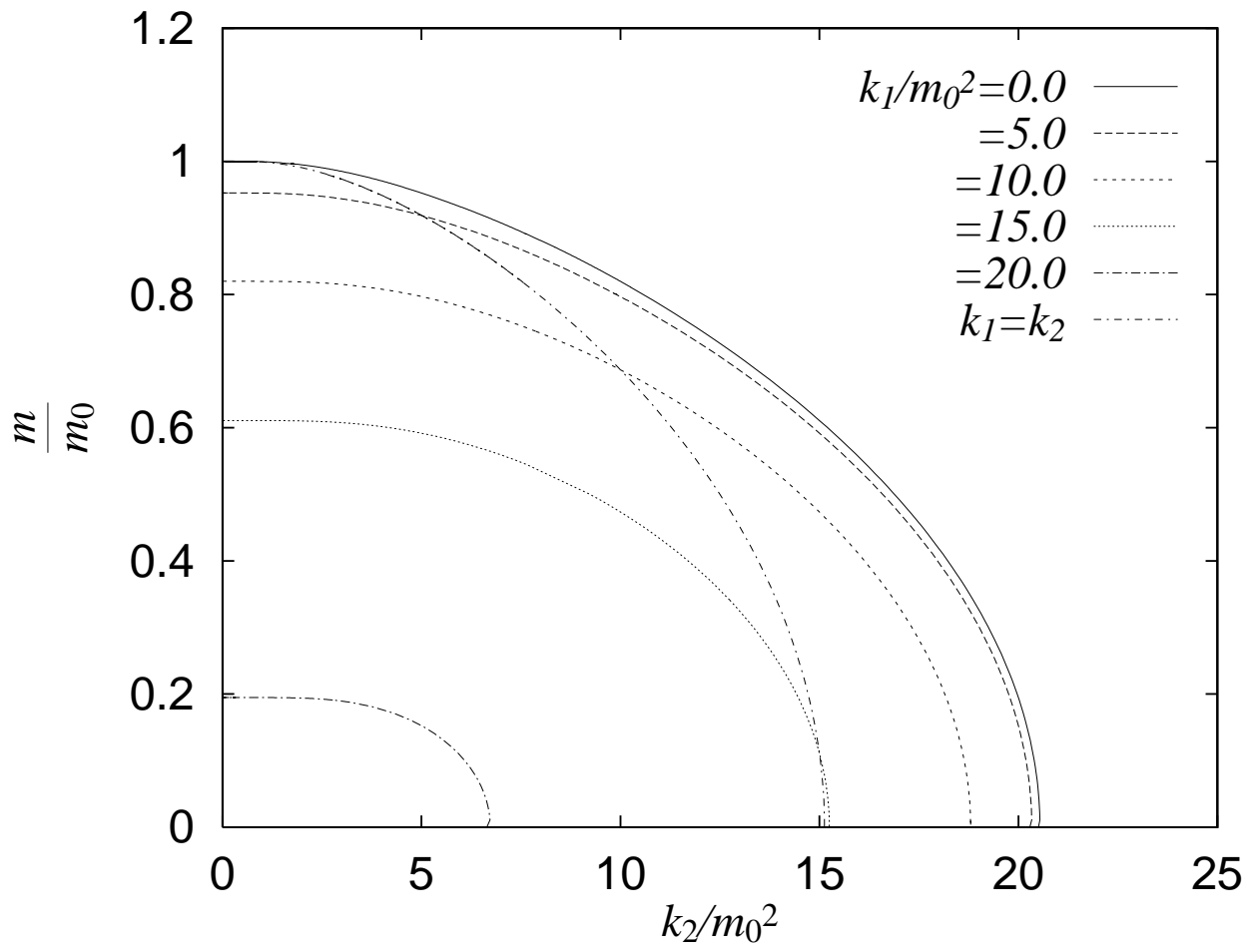


FIG. 1.

FIGURES

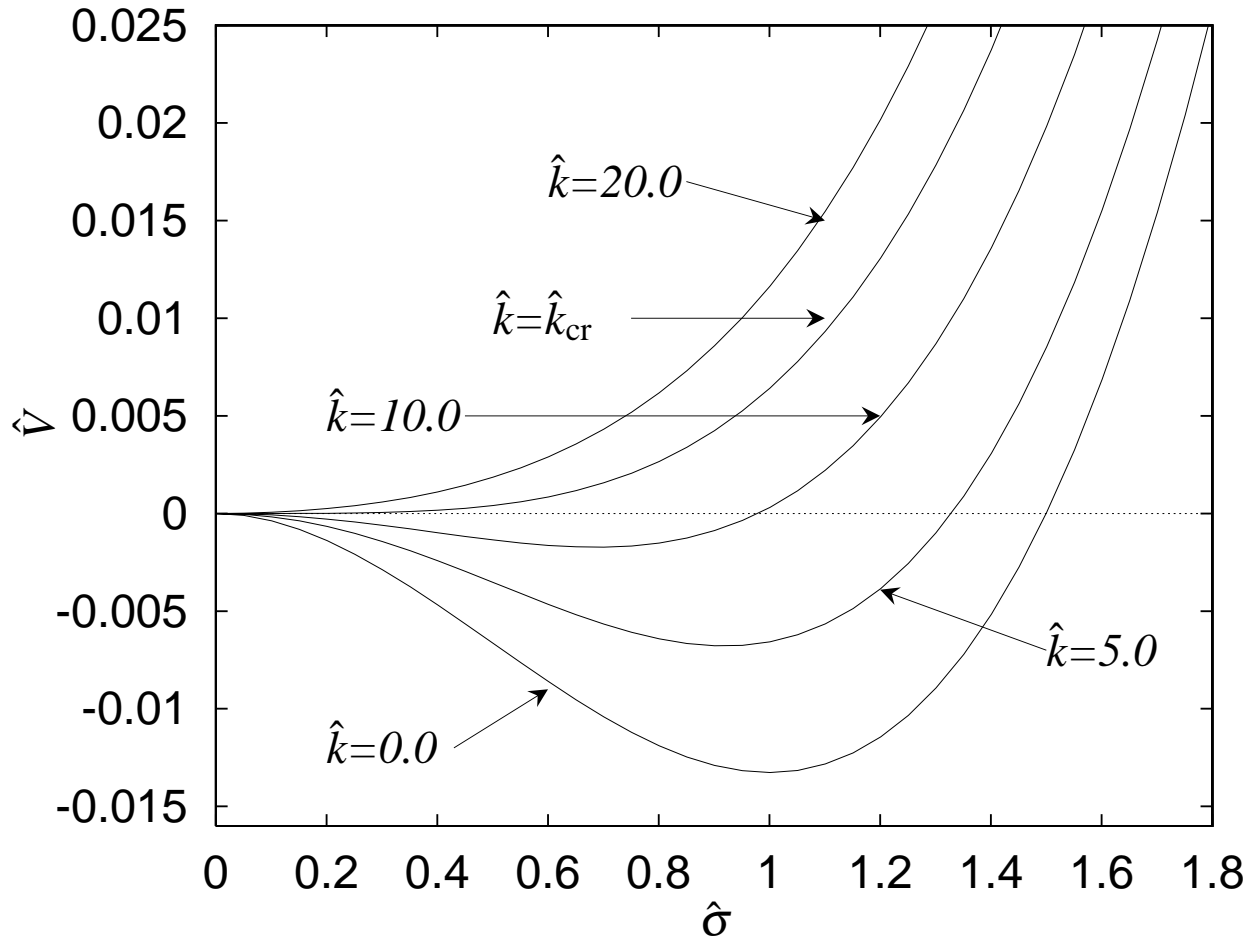


FIG. 2.

FIGURES

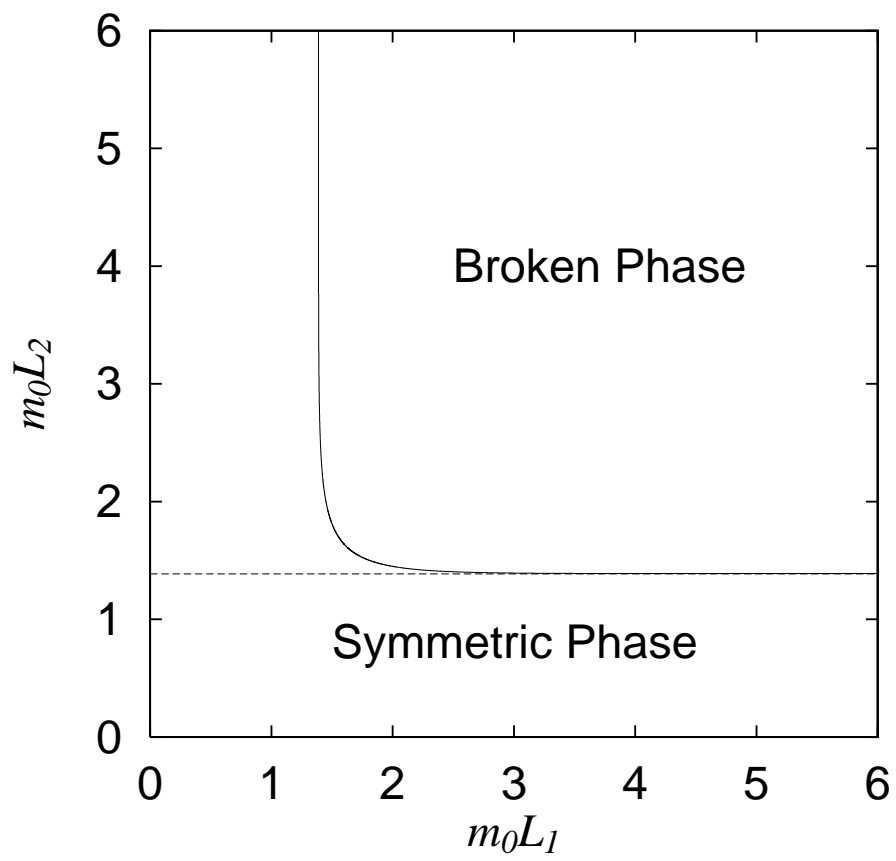


FIG. 3.

FIGURES

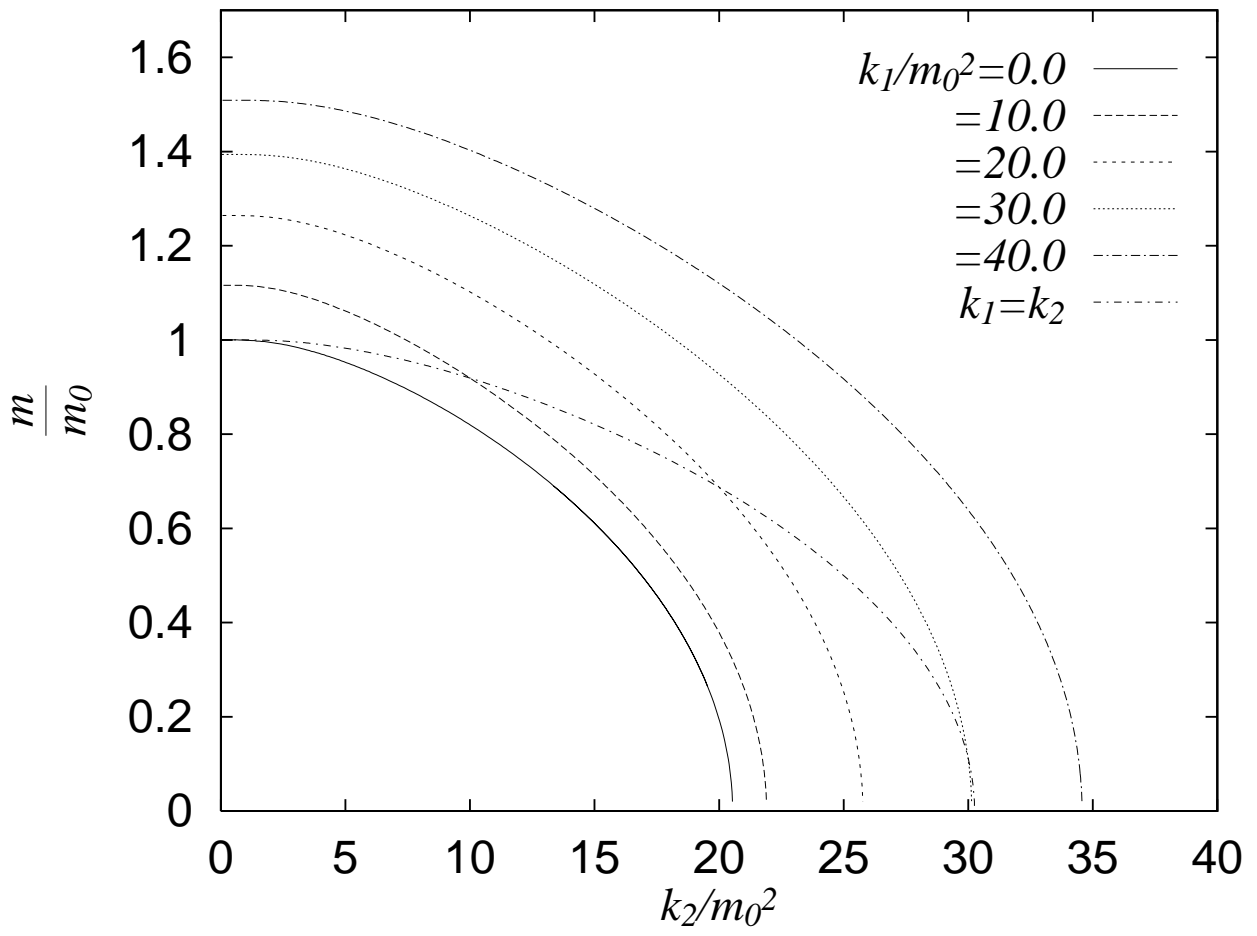


FIG. 4.

FIGURES

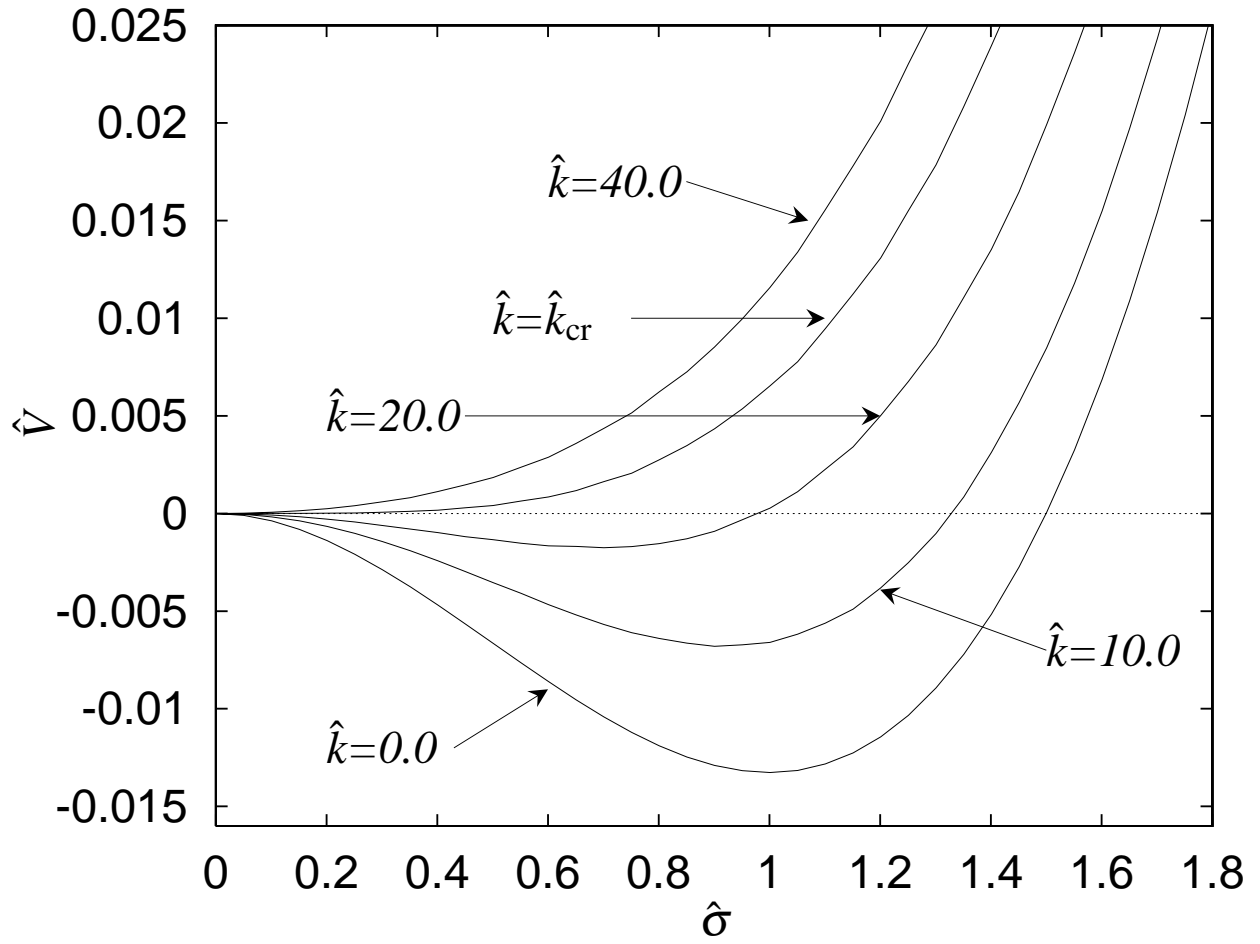


FIG. 5.

FIGURES

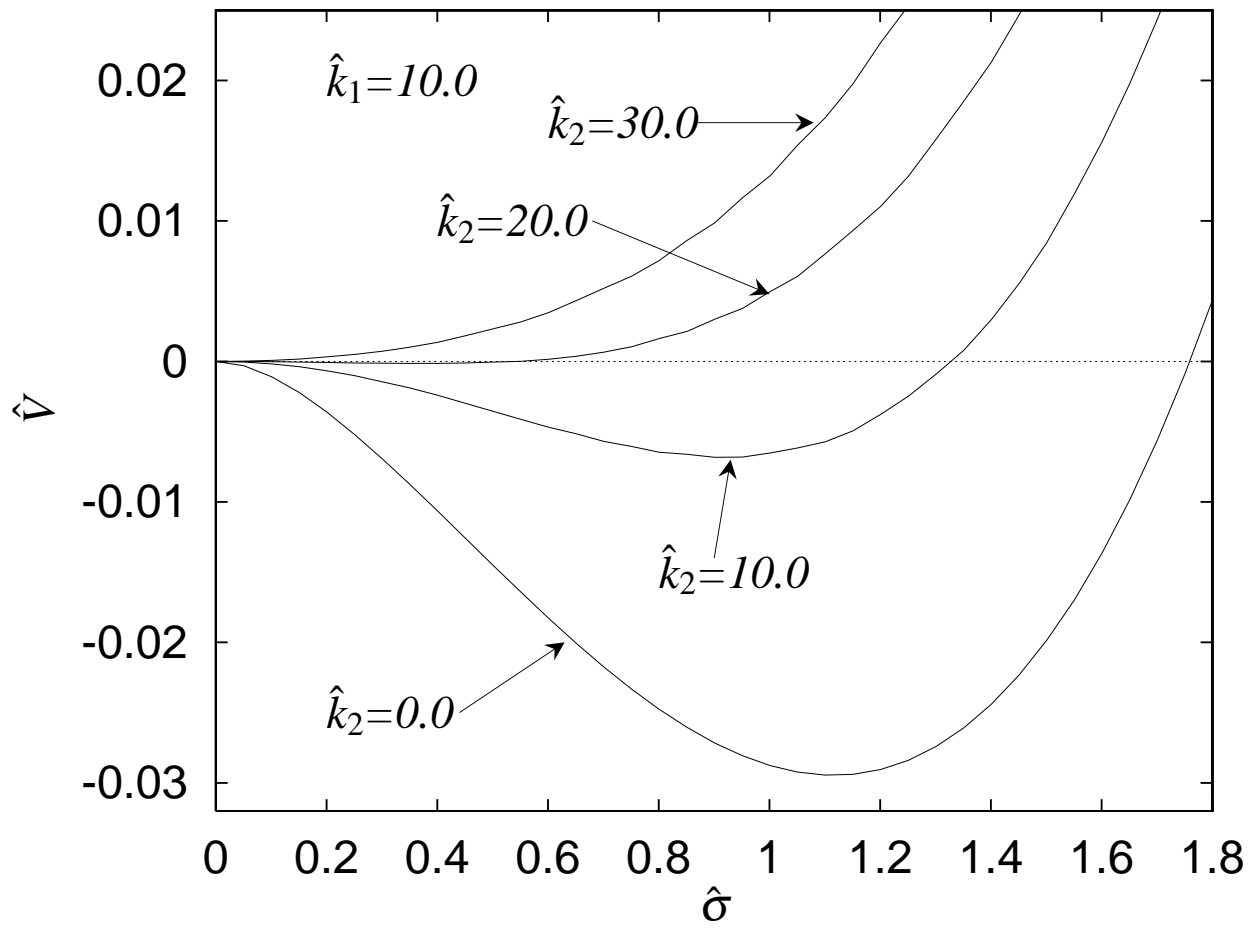


FIG. 6.

FIGURES

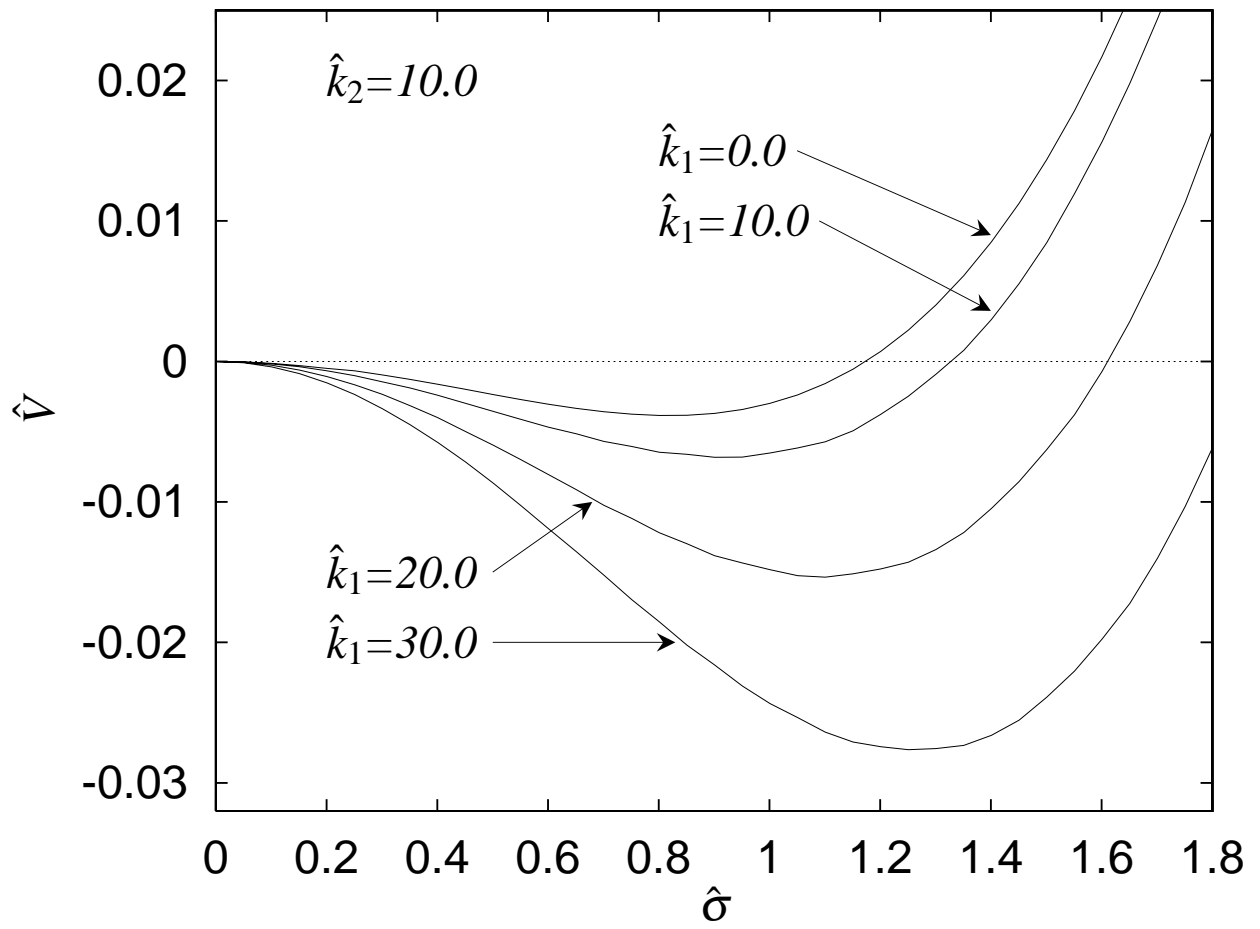


FIG. 7.

FIGURES

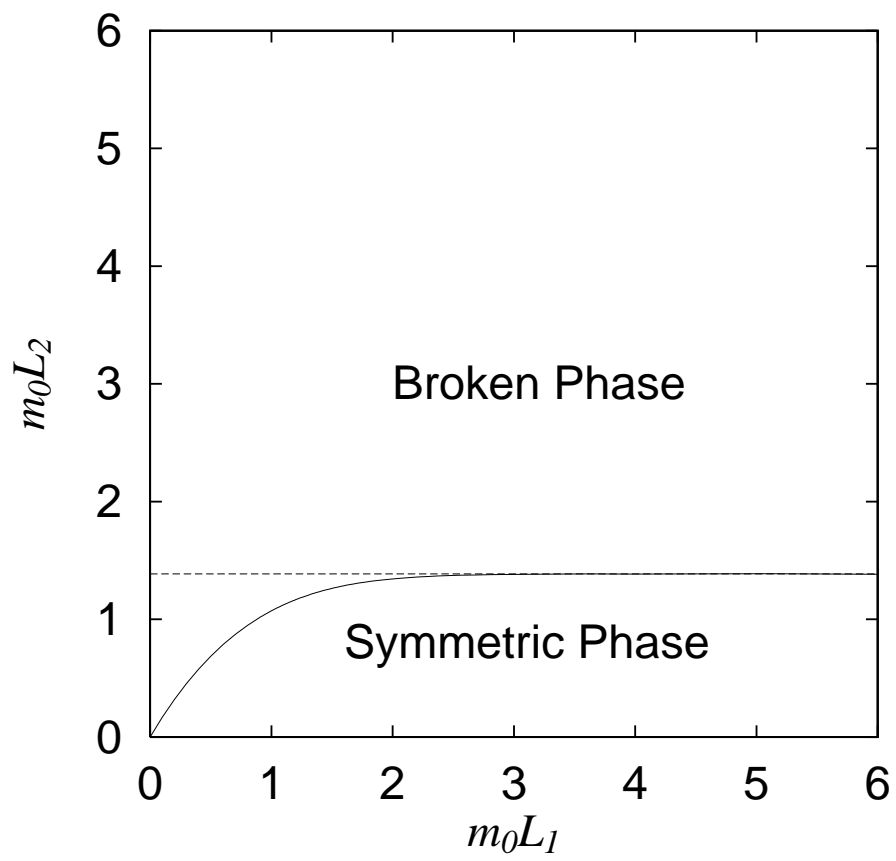


FIG. 8.

FIGURES

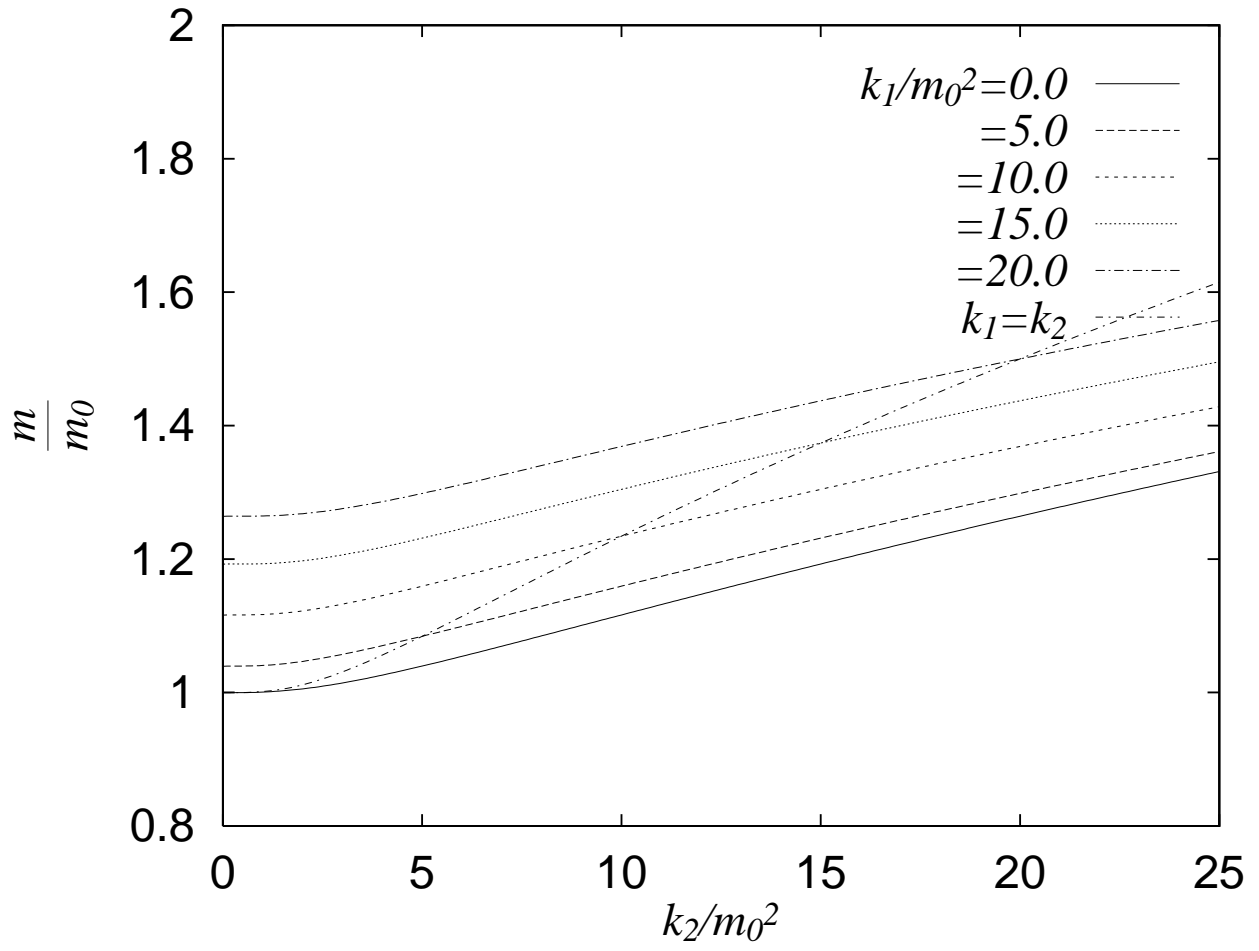


FIG. 9.

FIGURES

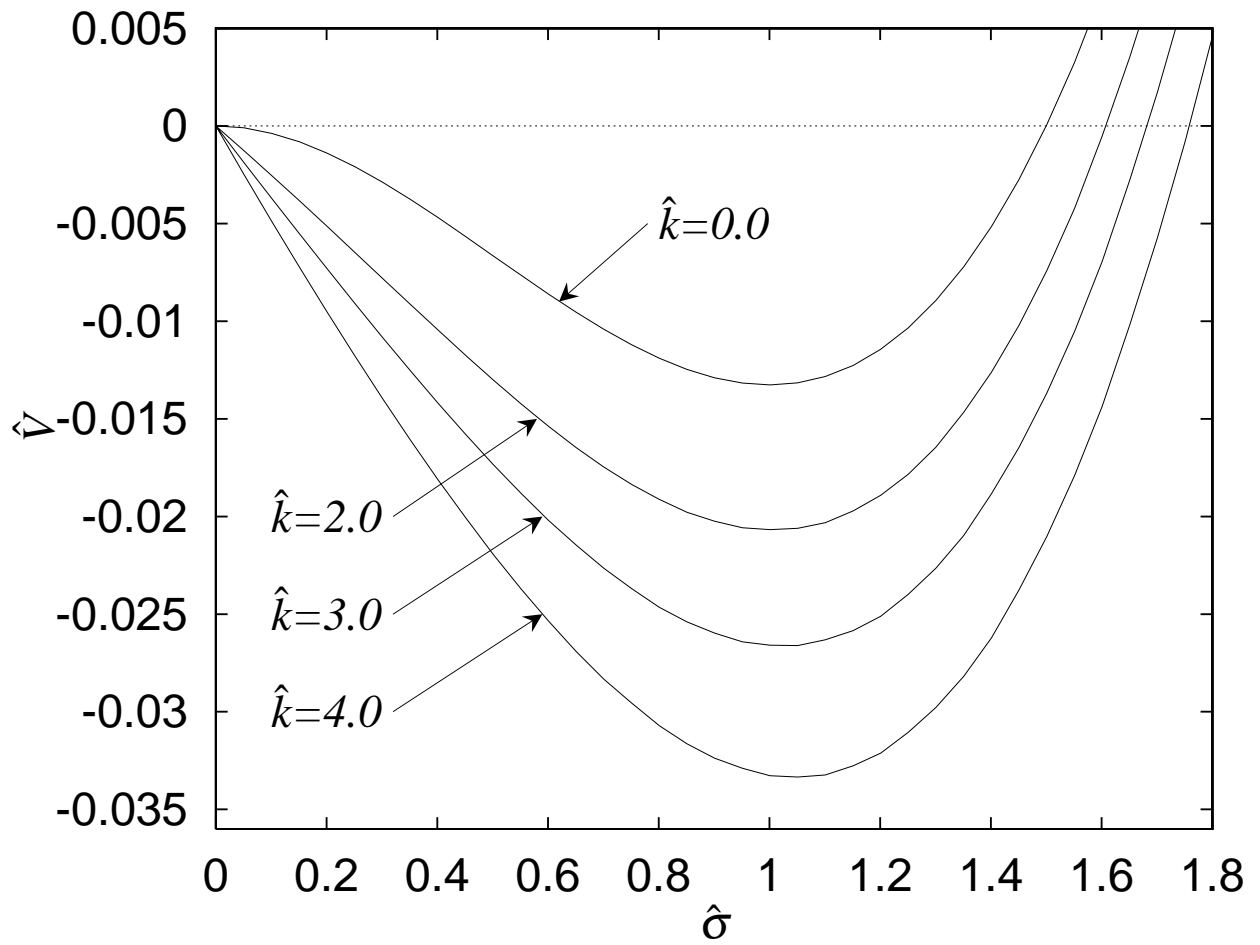


FIG. 10.

FIGURES

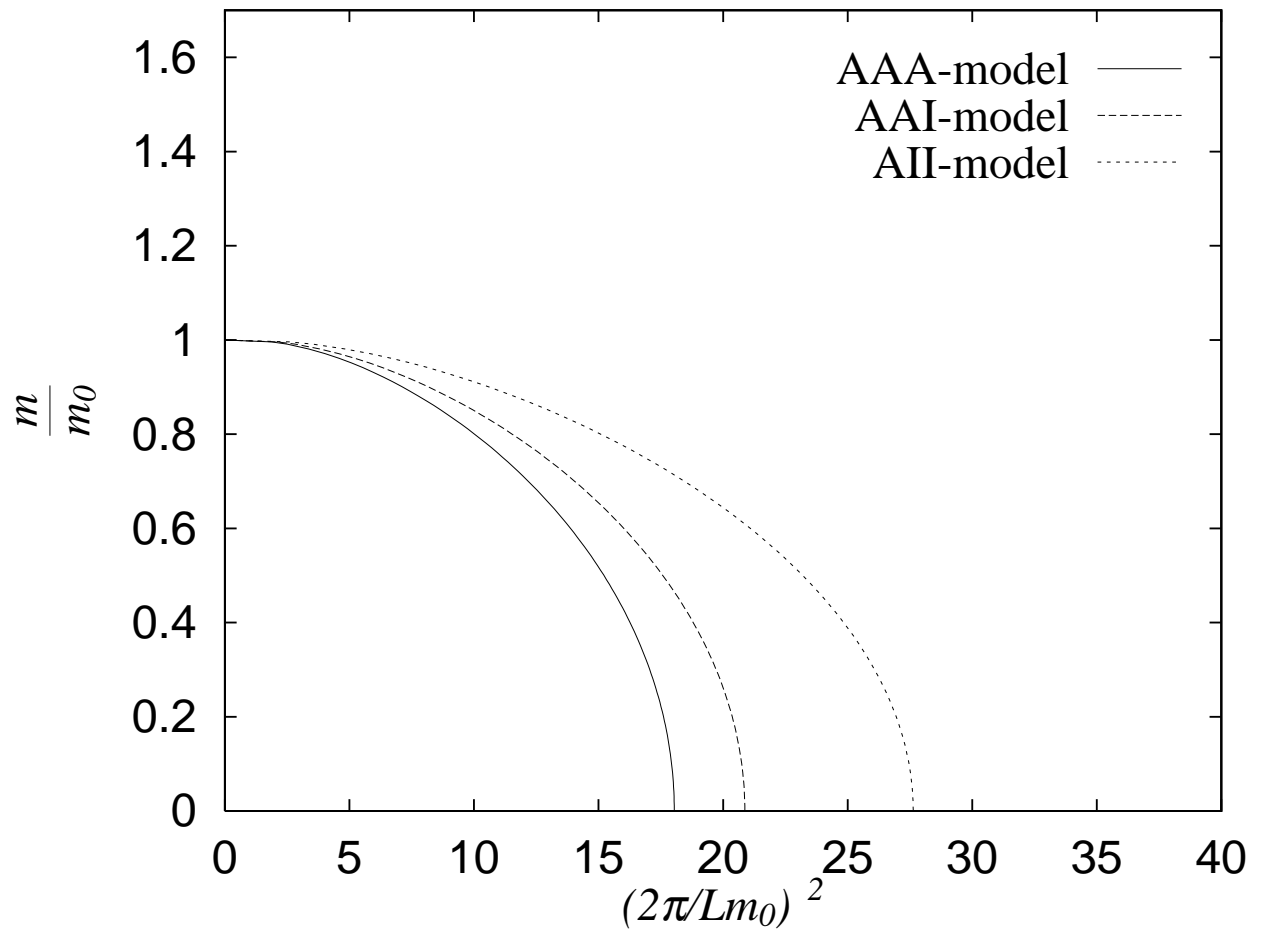


FIG. 11.

FIGURES

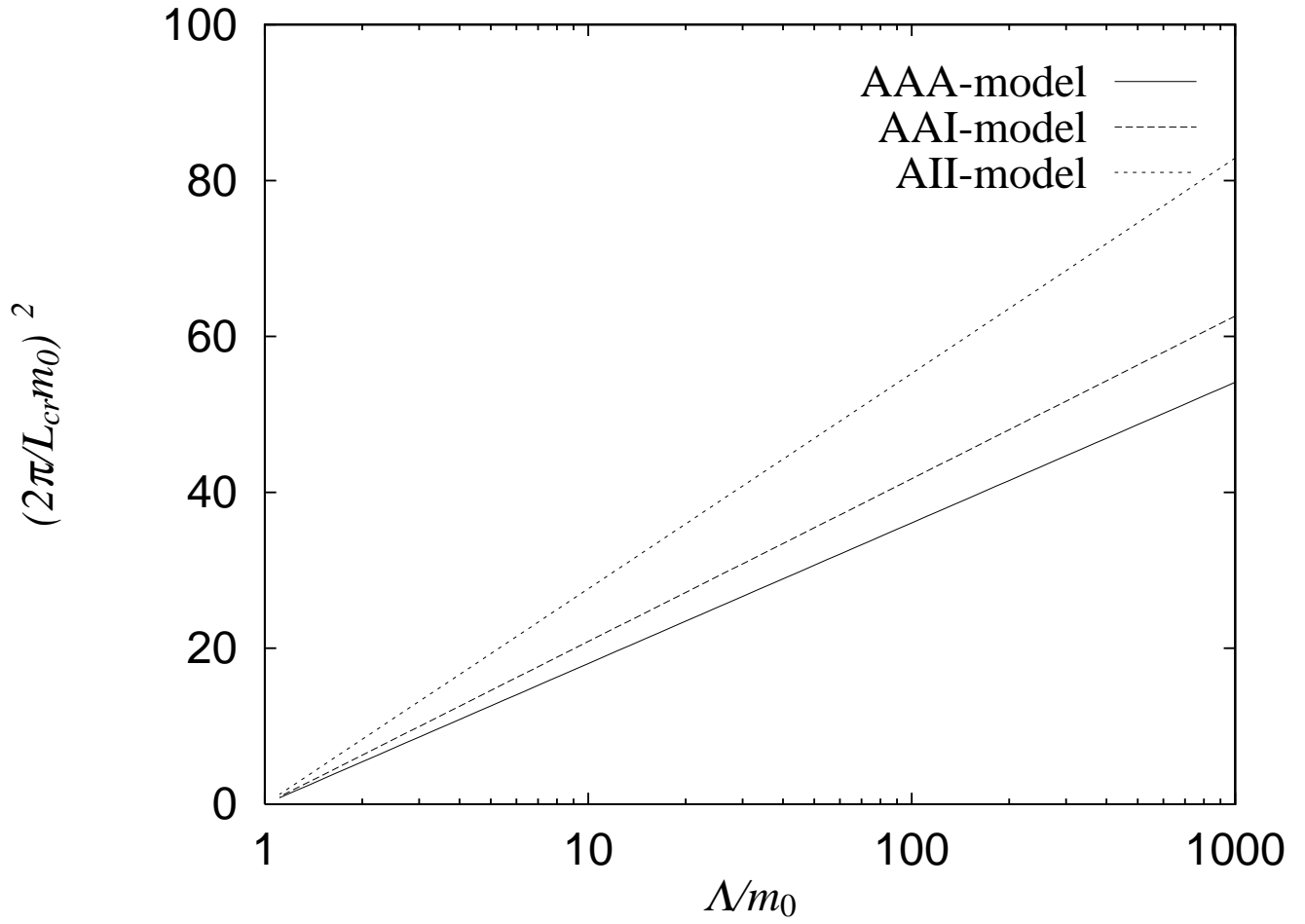


FIG. 12.

FIGURES

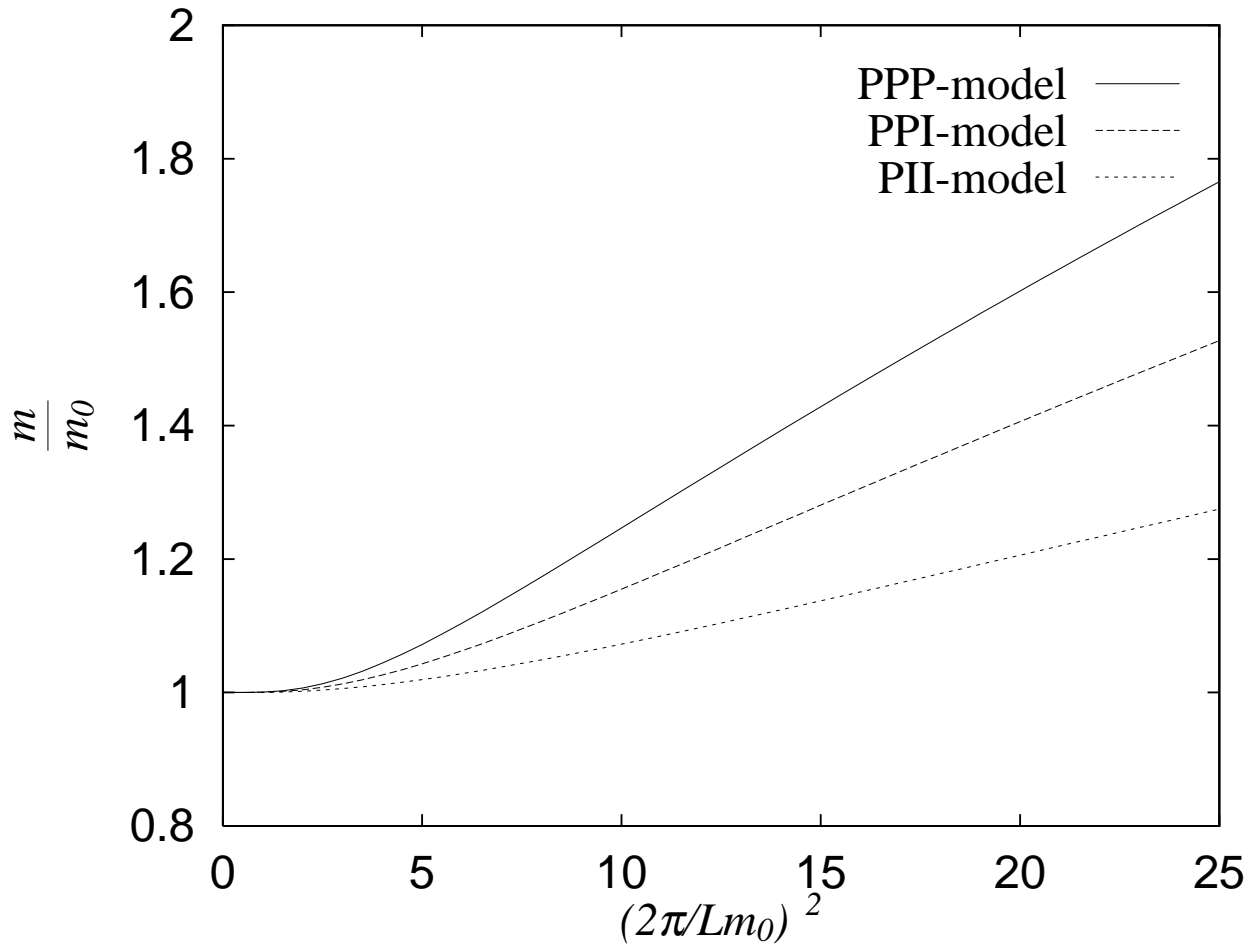


FIG. 13.

FIGURES

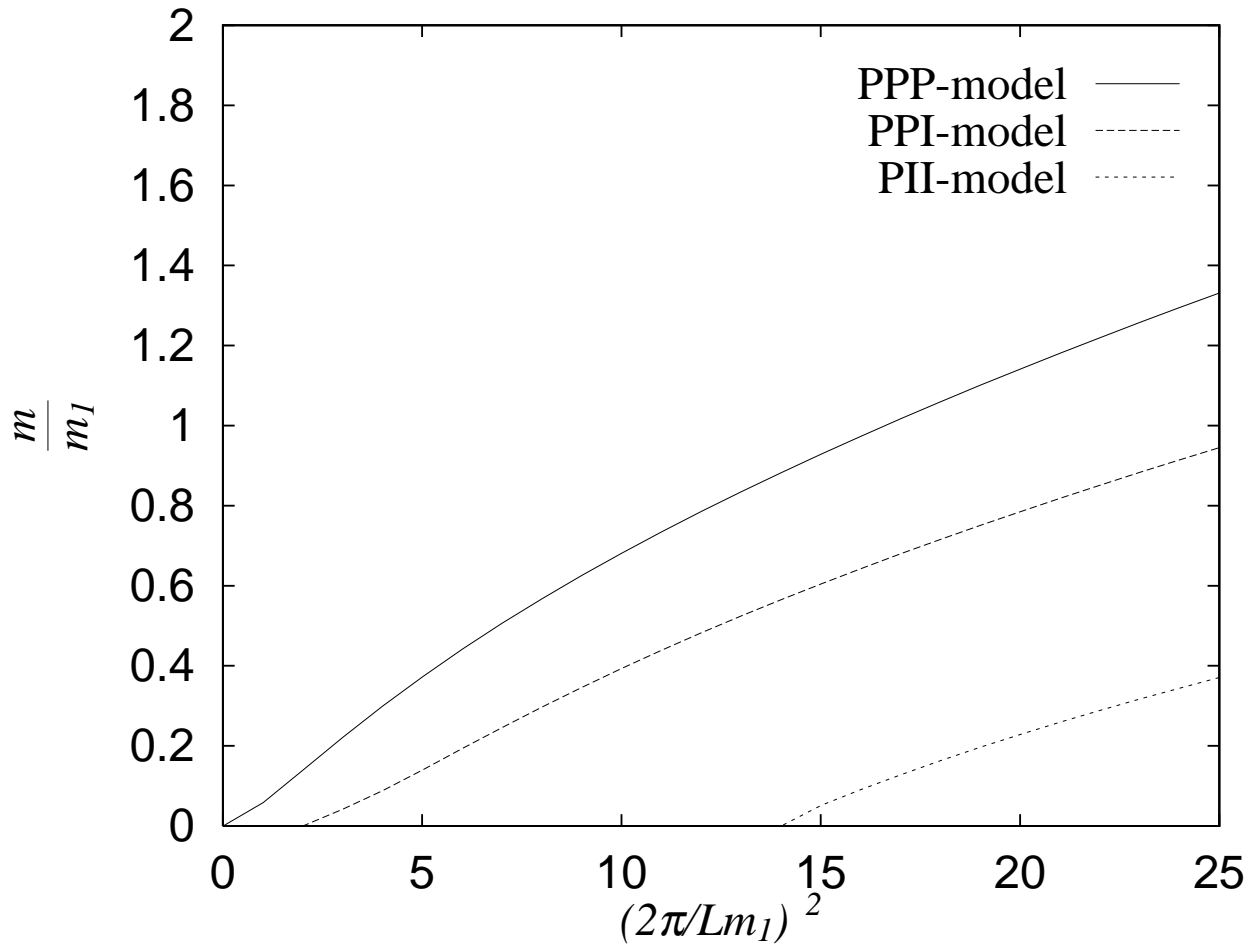


FIG. 14.

FIGURES

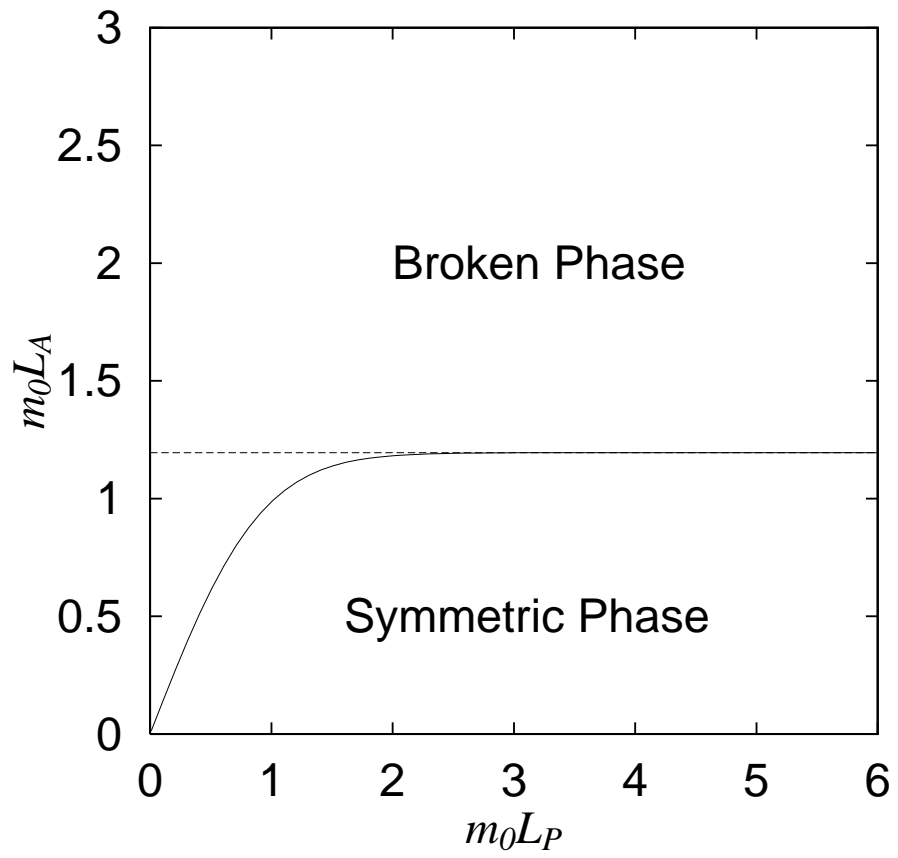


FIG. 15.

FIGURES

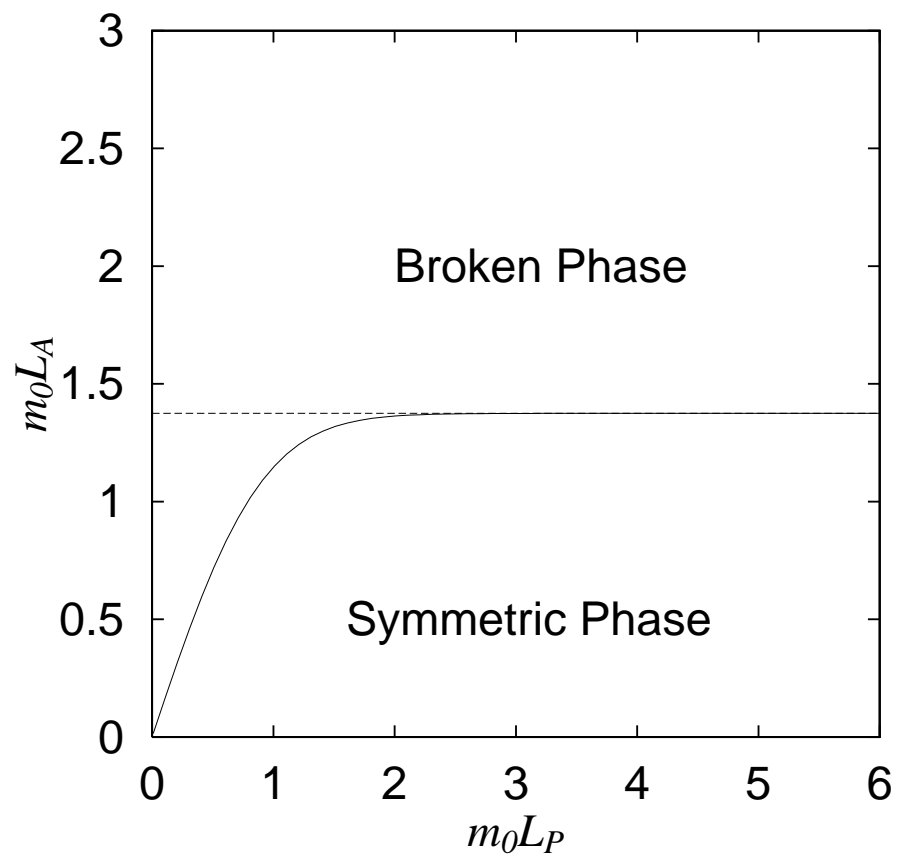


FIG. 16.

FIGURES

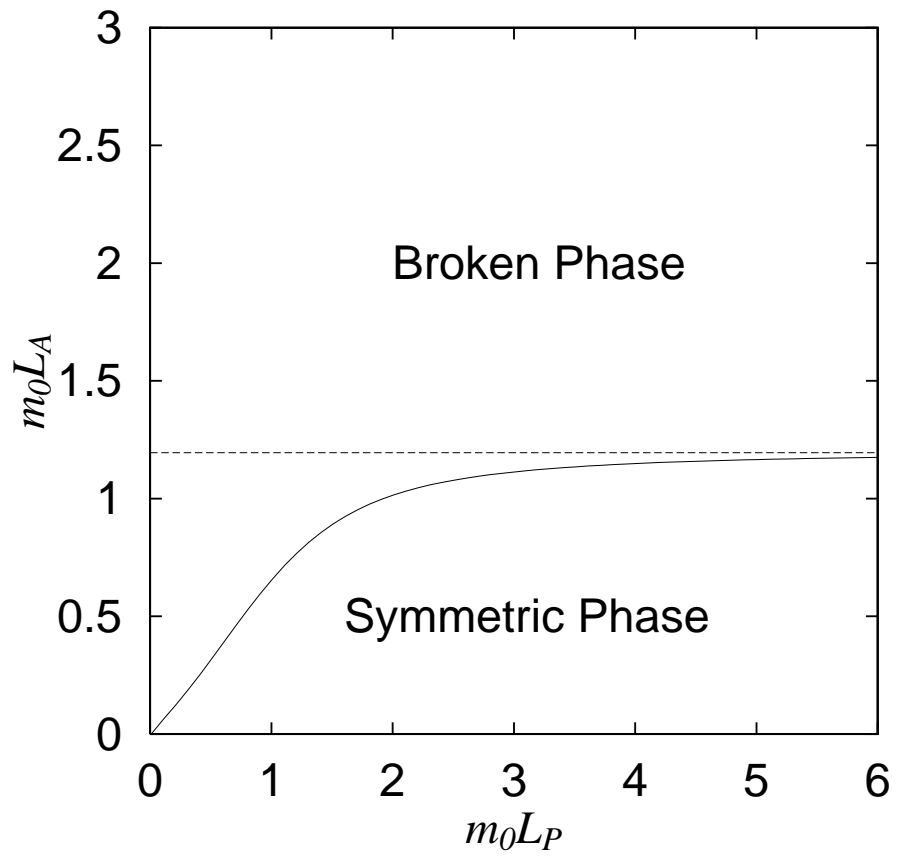


FIG. 17.